Materials Advances

ROYAL SOCIETY OF CHEMISTRY

REVIEW

View Article Online
View Journal | View Issue

Check for updates

Cite this: *Mater. Adv.*, 2023, 4, 5496

An insight into synthesis, properties and applications of gelatin methacryloyl hydrogel for 3D bioprinting

Rudra Nath Ghosh,[a] Joseph Thomas,[b] Vaidehi B. R.,[a] Devi N. G.,[a] Akshitha Janardanan,[c] Pramod K. Namboothiri[a] and Mathew Peter *[a]

Received 16th September 2023,
Accepted 13th October 2023

DOI: 10.1039/d3ma00715d

rsc.li/materials-advances

Bio-fabrication is an emerging area that involves the creation of tissue constructs with a hierarchical architecture. The essential requirements for fabricating a tissue construct are cells, biomaterial and bioactive molecules. Biomaterial selection is essential to support cell growth in a 3D microenvironment. Gelatin methacryloyl (GelMA) is a chemically modified form of gelatin biopolymer and has been extensively utilized for fabricating 3D tissue-engineered constructs. Photopolymerisation, thermal gelation or redox reaction are common methods to crosslink GelMA hydrogels. The ability of GelMA to undergo photopolymerisation is a promising aspect for tissue engineering since it facilitates the fabrication of dynamically tunable 3D crosslinked structures. As we see rapid advancement in tissue engineering and regenerative medicine, 3D bioprinting technology has paved the way for the fabrication of tissue constructs that can closely mimic the native tissue architecture. This review summarises the different methods for synthesizing GelMA and GelMA composite hydrogels and discusses their properties and applications in the field of tissue engineering. Further, the review focuses on applying GelMA hydrogel for fabricating various biomimetic tissues and organ constructs, such as cartilage, bone, cardiac tissue, skeletal muscle, and skin tissue, using a 3D bioprinting approach.

[a] *Department of Biomedical Engineering, Manipal Institute of Technology, Manipal, Manipal Academy of Higher Education, Manipal, India. E-mail: mathew.peter@manipal.edu*
[b] *Department of Plastic Surgery, Kasturba Medical College, Manipal, Manipal Academy of Higher Education, Manipal, India*
[c] *Manipal School of Life Sciences, Manipal, Manipal Academy of Higher Education, Manipal, India*

1. Introduction

Tissue engineering is a process that allows the fabrication of tissues and organs with the help of several growth factors and biocompatible polymers. With the advances in tissue

Rudra Nath Ghosh

Rudra Nath Ghosh received his BSc in Biotechnology (2014) and MSc in Molecular Biology and Human Genetics from the Manipal Academy of Higher Education and Universite Grenoble Alpes. He is currently pursuing his PhD work at the Department of Biomedical Engineering, Manipal Institute of Technology, Manipal under Manipal Academy Of Higher Education (MAHE). He was awarded a national scholarship from the Department of Biotechnology for his work that focuses on the development of biomicrofludics devices to understand cellular migration through different physiochemical gradients.

Joseph Thomas

Dr Joseph Thomas is currently an associate professor at the Department of Plastic Surgery, Kusturba Medical College, Manipal. He received his MBBS degree from Kasturba Medical College, Mangalore, and his MS and MCh in Plastic and Reconstructive Surgery from Government Medical College, Kozhikode-Kerala, India. He is currently heading the burns unit in KMC, Manipal and is part of two start-ups focused on negative pressure wound therapy devices and hydrogels for the treatment of burn wounds.

engineering techniques, damaged tissues such as bones, cartilage, skin, and blood vessels can be repaired or replaced.[1] An ideal tissue engineering system consists of three components: reparative cells, a functional matrix that acts as a scaffold to help in cell growth, proliferation and support, and bioactive molecules that support the formation of desired tissue, such as cytokines and growth factors.[2] Tissue engineering aims to overcome limitations of organ transplantation, such as the shortage of donors and the requirement for immunosuppressive therapy, and reduces the use of xenografts for *in vivo* testing by inducing tissue-specific regeneration processes. It also helps construct *in vitro* models of healthy tissues or organs, which can be used to evaluate therapies, screen drugs, and study the complex mechanism determining disease onset and progression.[3] Functional tissues can be developed by two tissue engineering approaches: the top-down and the bottom-up. In the top-down approach, a pre-fabricated artificial support matrix (a scaffold) is seeded with desired cells to form a tissue construct.[4] Although this technique holds many promises, a significant drawback of this approach is a failure to replicate native tissue architecture and geometries. Further, in this technique, it is not feasible to deposit multiple-cell types within the scaffold with the desired spatial orientation.[5] The second approach, the bottom-up approach or 3D bioprinting, is gaining popularity in tissue engineering.[6] In a bottom-up approach, cell-laden hydrogel is used to fabricate a tissue construct. Here, a hydrogel bio-ink and cells are loaded into a bioprinter, and with the help of computer algorithms, cell-laden hydrogels are printed in the desired spatial orientation and 3D geometry.[7] However, some limitations of this technique include failure to secrete extracellular matrix by cells, limited cell migration and inability to form cell–cell junctions. Further, if stem cells are incorporated into the 3D construct, they may differentiate into an undesired cell lineage depending on the hydrogel properties

Vaidehi B. R.

Vaidehi B. R. received her Bachelor's degree in Chemistry from St. Aloysius, Mangalore and her Master's degree in Organic Chemistry from University of Mysore. Currently she is pursuing her doctoral studies at Department of Biomedical Engineering, Manipal Institute of Technology, MAHE and have been awarded a national scholarship from University Grant Commission – Junior Research Fellow for her research work that focuses on 3D dynamically tunable photoswitch modified hydrogels to study changes in cell behaviour.

Devi N. G.

Devi N. G. received her BTech degree in Electronics and Communication Engineering from College of Engineering Kidangoor Cochin University of Science and Technology and her MTech degree in Biomedical Engineering from Manipal Institute of Technology, MAHE. She is currently working as a patent analyst at Dolcera Corporation.

Akshitha Janardanan

Akshitha J. received her BSc(H) degree in Forensic Science from Amity School of Forensic Sciences, Amity University and her Master's degree (MSc) in Genome Engineering from Manipal School of Life Sciences, Manipal University. Currently, she is working as a Genome Research Analyst (Oncology Dept) in Kyvor Genomics Inc. Her work is about feeding evidence-based biomarker data taken from the published clinical studies/trials, reputed guidelines and drug labels into the company's in-house pipeline, through which their products CANLYTx® and MEDLYTx generate reports for clinicians to understand the therapeutic options for the patient.

Pramod K. Namboothiri

Dr Pramod K Namboothiri is currently Assistant professor (selection grade) at the Department of Biomedical Engineering, MAHE. He received his MTech in Nanomedical Science from Amtita Vishwa Vidyapeetham, Ettimadi, India and PhD in Nanotechnology from Indian Institute of Technology, Bombay. He has Research experience of 12 years. And 7 years of Teaching experience. His area of expertise includes Polymer Science, Biomaterials, Nanomaterials and Nanotechnology.

Table 1 Comparison between top-down and bottom-up approaches in tissue engineering

Properties	Top-down approach	Bottom-up approach
Fabrication method	A predefined scaffold is used for seeding cells that will provide mechanical support to the cells.	Layer-by-layer deposition of biomaterial with cells in a desired shape and spatial orientation.
Cell types	Generally, a single cell type can be seeded to fabricate the tissue construct.	Multiple cell types can be used for fabricating complex tissue architecture.
Spatial orientation	Generally, cells seeded on top of the scaffold have low penetration. Desired spatial arrangements of cells are difficult to achieve with this approach.	Allows spatial arrangement of cells by layer-by-layer deposition/crosslinking.

and external environment.[8] Hence, the selection of a suitable hydrogel is essential to overcome these challenges. The comparison and differences of the two approaches in tissue engineering are summarized in Table 1.[9]

1.1. Hydrogels

Hydrogels are polymeric materials derived *via* crosslinking of monomer units to form a crosslinked 3D network and have a good water-holding capacity.[10] For tissue engineering applications, hydrogels are essential in providing an artificial extracellular matrix microenvironment for cells and tissues. Crosslinking between the polymeric units of the hydrogel determines the structural integrity and other physical parameters of the 3D construct.[11] The different crosslinking strategies used for fabricating 3D hydrogel constructs are highlighted in Fig. 1. Physical parameters such as mechanical properties, pore size, and gel strength are essential for tissue engineering applications. The hydrogel must be biocompatible so that the cells can proliferate and form a tissue construct.[12] Hydrogels used for bioprinting can be made from synthetic or natural polymers. Further, natural and synthetic-derived polymers can be blended to fabricate 3D tissue construct with optimized physio-chemical, biological, and mechanical properties.[13,14]

1.2. Gelatin methacryloyl (GelMA)

This review focuses on the synthesis, properties, and application of gelatin methacryloyl (GelMA) hydrogel for tissue engineering, focusing on 3D bioprinting application. The primary constituent of GelMA hydrogel is gelatin. Gelatin is a collagen derivative derived from the hydrolysis of collagen, which breaks the natural triple-helix structure of collagen. Gelatin has been extensively used in tissue engineering due to its excellent biocompatibility and thermal gelation to form gels.[15] Gelatin hydrogel has also been used as a carrier molecule for delivering drugs and growth factors in tissue engineering.[16–18] The chemical alteration of gelatin to prepare GelMA is carried out by adding methacrylic anhydride that modifies the lysine and hydroxyl residues by introducing methacrylamide and methacrylate side groups.[19] The methacryloyl modification of gelatin does not affect essential properties like reversible thermal gelation and RGD (arginine–glycine–aspartic acid) motif required for cell adhesion.[20] GelMA hydrogel is a hydrophilic polymer and provides an aqueous environment that supports cell growth and proliferation. When subjected to UV light, the chemically modified GelMA with methacryloyl side group undergoes rapid polymerisation by crosslinking of the methacryloyl backbone, and this is useful for cell encapsulation and for developing 3D tissue construct.[21] Photoinitiators like lithium phenyl-2,4,6-trimethyl-benzoyl phosphinate (LAP) and 2-hydroxy-4′-(2-hydroxyethyl)-2-methylpropiophenone (Irgacure-2959) are generally used for photopolymerisation

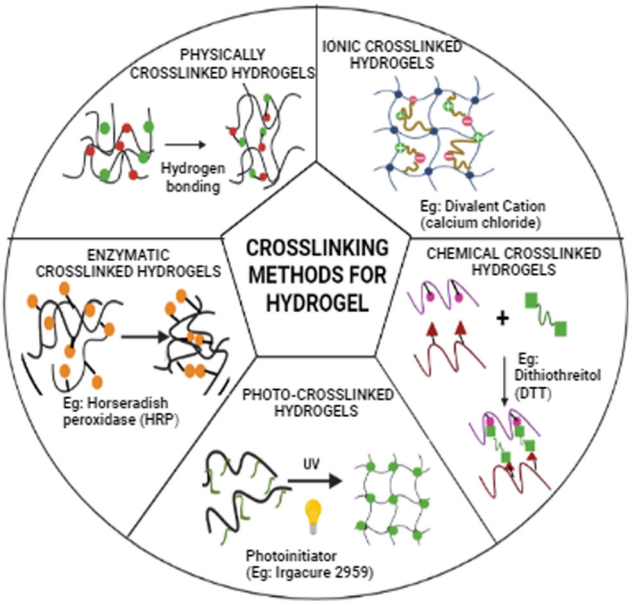

Fig. 1 Schematic representation of different crosslinking strategies for fabrication of 3D hydrogel construct. The diagram depicts the different physical crosslinking and chemical crosslinking techniques.

Mathew Peter

Dr Mathew Peter is currently an Assistant professor at the Department of Biomedical Engineering, Manipal Institute of Technology, MAHE. He received his M.Tech. in nanomedical science from Amrita Vishwa Vidyapeetham, Ettimadi, India and PhD in Biomedical Engineering from the Indian Institute of Technology, Bombay. His research interest mostly deals with nanoparticles, three dimensional cell culture, biomaterials and tissue engineering.

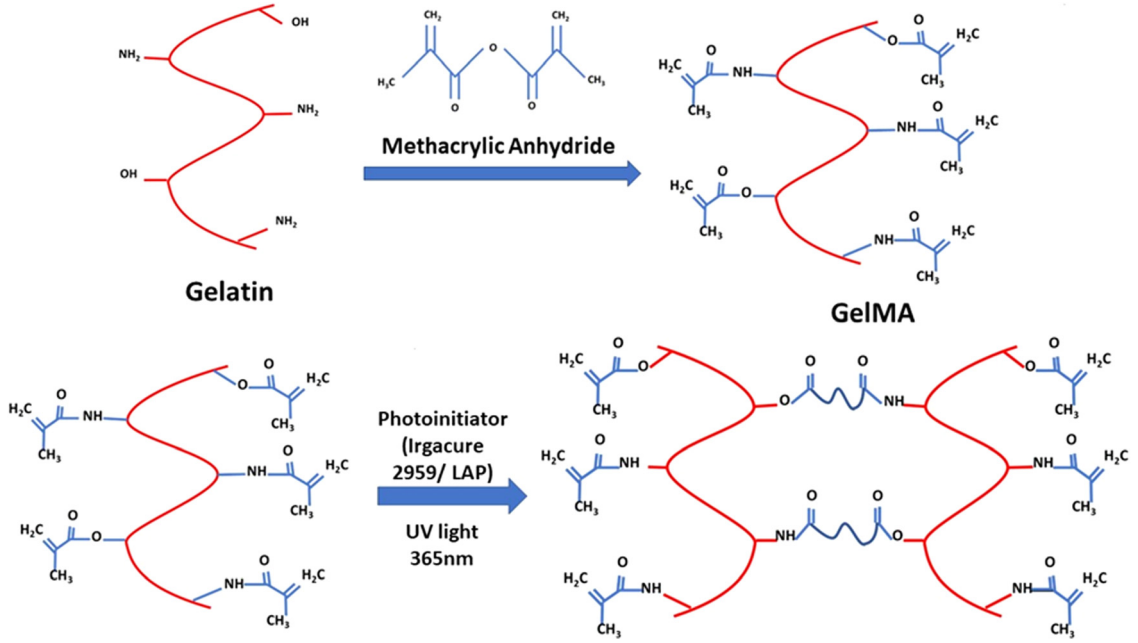

Fig. 2 The schematic of the synthesis of GelMA synthesis and crosslinking.

and initiate photopolymerisation upon the release of free radical.[22] The mechanical properties and cell viability of crosslinked GelMA depend upon three critical factors discussed in the following sections.[23] The chemical modification of gelatin with methacrylic anhydride (MA) to form GelMA polymer and the crosslinking of GelMA to form 3D hydrogels by photopolymerisation is illustrated in Fig. 2.

1.2.1. Effect of GelMA concentration and matrix stiffness. The concentration of GelMA determines the extent of crosslinking between methacryloyl side groups, directly influencing the gel stiffness (matrix stiffness). With a higher concentration of GelMA, more methacryloyl side groups are crosslinked, resulting in a higher degree of crosslinking. In literature, GelMA concentration used for cell-based studies varies from around 3–30% w/v. Cell encapsulated in lower concentration GelMA results in better cell viability due to a decrease in matrix stiffness.[24–27] The degree of crosslinking is further governed by photoinitiator concentration and light intensity. In a study performed by Wu *et al.*, a GelMA hydrogel was prepared with varying stiffness to understand its influence on neuronal outgrowth by seeding PC12 cells. A range of GelMA concentrations (5–30% w/v) was selected for seeding PC12 cells, demonstrating GelMA hydrogel's biocompatibility. The results showed that as the GelMA concentration was increased, a significant decrease in cell adhesion was observed. Higher cell viability, cell spreading and neurite length were observed with a 10% w/v GelMA concentration with Young's modulus of 34.90 kPa, which was found to be optimal for neuron regeneration.[28] Lin *et al.* demonstrated the role of stiffness of GelMA hydrogel matrix on endothelial differentiation of mesenchymal stem cells (MSCs). Different concentration of GelMA (5%, 10% and 15% w/v) was used to prepare gels with varying stiffness and MSCs were seeded in GelMA with EGM-2 endothelial cell differentiation media. The differentiation of MSCs to endothelial cells was observed with softer gels having a matrix stiffness of 25.59 ± 2.09 kPa (5% w/v GelMA) or 33.69 ± 1.13 kPa (10% w/v GelMA) compared to stiffer gels having a matrix stiffness of 41.78 ± 1.10 kPa (15% w/v GelMA), which was quantified using different molecular techniques and cell surface markers.[29] Another study by M. Costantini *et al.* GelMA hydrogels were prepared by varying polymer concentrations (3, 4, 6 and 8% w/v) to understand the myotube formation of C2C12 myoblast cells within the polymerized GelMA matrix. The results depicted that at a lower GelMA concentration (3% w/v and 4% w/v) having an elastic modulus of 1.19 ± 0.12 kPa and 3.20 ± 0.10 kPa respectively, a large number of myotube formations were observed, whereas only a smaller number of myotube formation was seen with a higher concentration of GelMA (6% w/v and 8% w/v) having an elastic modulus of 8.74 ± 0.22 kPa and 16.55 ± 0.80 kPa respectively.[30] Interestingly, GelMA concentrations and matrix stiffness can be used to modulate cell adhesion, proliferation, and differentiation. Cell behaviour and properties are not only dependent on GelMA concentration but also influenced by the cell types. Generally, a stiffer GelMA matrix has a negative effect on cell viability, growth and proliferation. The optimum GelMA concentration used for various cell studies and bioprinting lies between 5–10% w/v. Lower GelMA concentration below 5% w/v may not form gels or may form weak gels, which may not be suitable for tissue engineering application.

1.2.2. Effect of photoinitiator type and concentration. GelMA hydrogels are photo-polymerised *via* chain propagation through free radical-based crosslinking. The free radical is generated from a photoinitiator molecule upon excitation with

a particular wavelength of light. The generated radical is then transferred to the methacryloyl group of GelMA macromers, forming a covalent linkage between two methacryloyl side groups.[31] Free radical generation from different photoinitiators depends on specific wavelength light irradiation. The selection of photoinitiators is critical for efficient photo-polymerisation. A photoinitiator should have a broad excitation spectrum and high efficiency to generate free radicals. Based on the free radical generations mechanism, photoinitiator systems are classified into type I and type II.[31] Type I photoinitiators consist of peroxides, per-esters, iminosulphones, or ketones groups that are cleaved to generate free radical molecules upon excitation with a specific wavelength of light and help in chain propagation during photopolymerisation. Type II photoinitiator system consists of a photosensitiser (initiator) and a co-initiator molecule that is generally excited using a visible light spectrum. The photosensitizer reacts with the co-initiator on light irradiation to release free radicals by donating or accepting an electron from a co-initiator molecule. Light irradiation generally releases a cationic radical from the photosensitiser and an anionic radical from the co-initiator. Alternatively, it may also result in an anionic radical from the photosensitiser and a cationic radical from the co-initiator.[32] The photopolymerisation process is slower with type II photoinitiator than with type I photoinitiator due to the back electron transfer process between the photosensitiser and co-initiator, oxygen inhibition and interaction with solvent or biomolecules.[33] Two-photon polymerization is another method for polymerizing hydrogels based on non-linear optical processes that rely on the photopolymer's simultaneous absorption of two photons. Two-photon photopolymerisation photinitiators are required to have a high two-photon absorption coefficient and are generally irradiated with an infrared light laser source. The photoinitiator in a two-photon system is characterised by π – bonding with a strong donor–acceptor group. Upon absorption of two photons by a photoinitiator, an electron is transferred from the donor–acceptor group to π – bonded group. Further, a transfer of electrons takes place between the photoinitiator and monomer, generating a radical that can initiate photopolymerisation.[34] The mechanism by which different types of photoinitiator undergoes bond dissociation to facilitate photopolymerisation is illustrated in Fig. 3. The most commonly used photoinitiators for photopolymerisation are summarised in Table 2.

A significant limitation of free-radical-mediated photopolymerisation is the presence of oxygen within the hydrogel system. The free radical binds to free oxygen molecules to form oxide derivates, thus reducing photopolymerisation kinetics.[57] Hence, it is suggested that photopolymizable hydrogels be degassed and photopolymerised under a reduced oxygen environment. Type I photoinitiators are preferred over type II because they form free radicals efficiently. One of the most common type I photoinitiators, which shows low toxicity for tissue engineering applications, is 1-[4-(2-hydroxyethoxy)-phenyl]-2-hydroxy-2-methyl-1-propanone, known as Irgacure 2959 (I2959). Irgacure 2959 releases free radicals upon excitation with UV light of wavelength 365 nm.[58] One of the significant drawbacks of the Irgacure photocuring system is the use of UV light to generate free radicals. Exposure to UV light can cause oxidative DNA damage by reacting with oxygen to produce reactive oxygen species (ROS), leading to mutagenicity and cell death.[59] Several other visible light photoinitiator

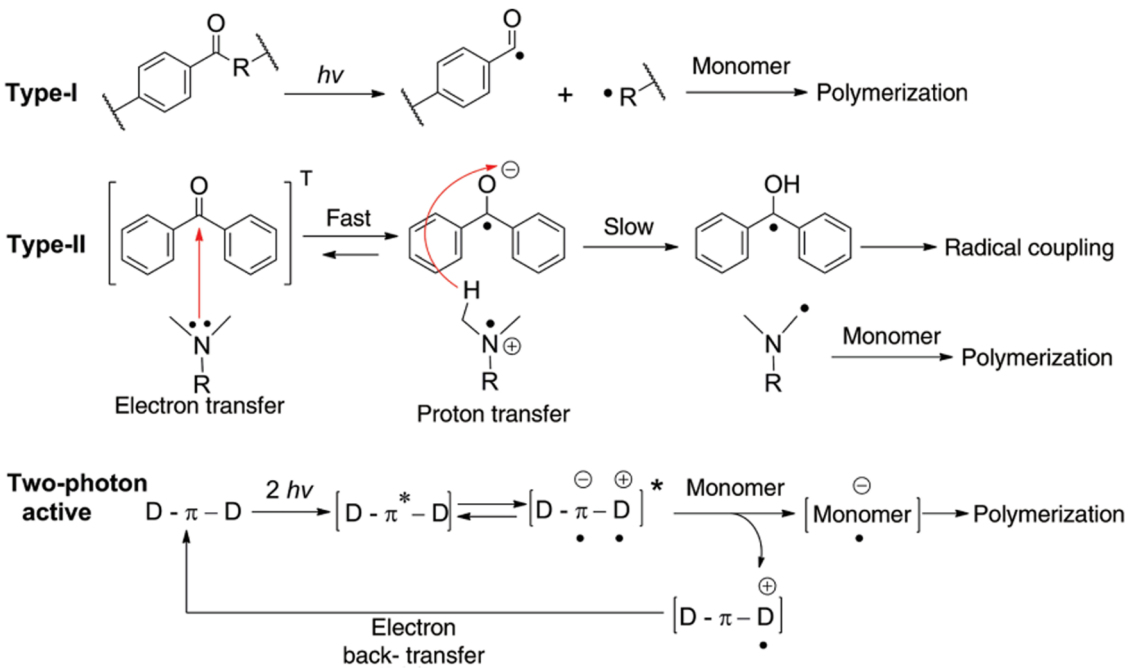

Fig. 3 Types of photoinitiator systems and their mechanism of free radical generation. Reproduced from ref. 35 with permission from De Gruyter, copyright (2014)

Table 2 Summary of photoinitiator used in photo-polymerisation

Type I

Photoinitiator	Irradiation wavelength	Photoinitiator concentration	Properties	Ref.
Irgacure 2959	UV, 365 nm	0.05–0.7% w/v	Low cytotoxicity, Low water solubility.	36–39
LAP	Visible, 405 nm	0.05–0.5% w/v	Water soluble, non-cytotoxic	39–42
VA-086	UV, 365–385 nm	0.5–1.5% w/v	Water soluble, non-cytotoxic	43–45

Type II

Photoinitiator system	Irradiation wavelength	Photoinitiator concentration	Properties	Ref.
Initiator: Eosin Y Co-initiator: triethanolamine (TEOA) and a comonomer: 1-vinyl-2 pyrrolidinone (NVP)	Visible, 400–800 nm	0.005–0.1 mM	Highly water-soluble, wide irradiation wavelength, non-cytotoxic	46–49
Initiator: camphorquinone co-initiator: tertiary amines (*e.g.* ethyl-4-dimethylaminobenzoate (EDAB)), heteroaromatic thiols (imidazole, oxazole, and thiazole derivatives)	Visible, 400–500 nm	150–600 mM	Wide irradiation wavelength, low water solubility.	50–52

Two-photon polymerization

Photoinitiator	Irradiation wavelength	Photoinitiator concentration	Properties	References
Distyrylbenzene chromophore (WSPI)	Laser, 800 nm	0.5–4% w/v	Focal point polymerisation with high resolution, good water solubility, non-cytotoxic	53–55
Benzylidenecycloketones (G2CK and P2CK)	Laser, 800 nm	1.827 mM	Focal point polymerisation with high resolution, good water solubility, non-cytotoxic	53 and 56

systems have been researched for photopolymerisation to overcome the negative effect of UV photocrosslinking. Lithium phenyl-2,4,6-trimethylbenzoylphosphinate (LAP) is a type I photoinitiator that behaves similarly to Irgacure 2959 by generating free radicals through bond cleavage upon excitation with visible light of wavelength 405 nm.[60] In a study by Xu *et al.*, photocrosslinking of GelMA was performed with two photoinitiators Irgacure 2959 and LAP, to understand the cell viability, physical properties and structural fidelity in a 3D bioprinted cellular GelMA construct. It was observed that cell viability decreases with an increase in photoinitiator concentration and printing time. Reduced cell viability was observed with increased Irgacure 2959 concentration (0.3% w/v to 0.9% w/v) than with LAP concentration (0.3% w/v to 0.9% w/v). The physical properties of photopolymerised GelMA cured with Irgacure 2959 showed larger pore size, faster degradation rate and higher swelling ratio when compared to LAP.[61] In a study performed by Khoon *et al.*, GelMA photopolymerisation was performed using a new photoinitiator system containing ruthenium (Ru) and sodium persulphate (SPS) crosslinked under a visible light wavelength range of 400–450 nm. Upon excitation, Ru^{2+} oxidises to Ru^{3+} and donates an electron to SPS, which undergoes dissociation into sulphate ions and sulphate radical that facilitates polymer crosslinking. The photocrosslinking of the Ru/SPS system was compared with Irgacure 2959 and LAP photoinitiators. The Ru/SPS system showed mechanical and physiochemical properties similar to gels crosslinked with Irgacure 2959 or LAP. However, better cell viability and cellular metabolic activity were observed with the Ru/SPS system compared to gel crosslinked with Irgacure 2959 or LAP.[31] Photo absorbers have also been explored to improve photopolymerization by visible light irradiation. In a study by Gugulothu and Chatterjee, 4D bioprinting was explored with GelMA and poly(ethylene glycol)dimethacrylate (PEGDM) bioink using DLP bioprinter which changes the shape upon hydration of the printed construct. A bioink formulation with 2.5% w/v PEGDM, 12.5% w/v GelMA, 0.2% w/v LAP and 1 mM tartrazine (used as photoabsorber) was bioprinted at 405 nm irradiation. The shape-changing kinetics of the 3D construct on hydration was studied by bioprinting rectangular flat sheets having different thicknesses. It was observed that shape change was faster in 0.6 mm sheets (5 min) compared to that of 1.2 mm sheets (15 min).[62] The mentioned studies here highlight the importance of the choice of photoinitiator system and concentration and the influences of these parameters on cell viability, mechanical properties and degradation, which are essential considerations for fabricating tissue constructs.

1.2.3. Light intensity. Light intensity is an important factor determining the photopolymerisable system's reaction kinetics. With increased light intensity, a faster crosslinking occurs by releasing more free radicals from the photoinitiator for the photopolymerisation reaction.[63] Generally, the UV light intensities for photocuring of GelMA ranges from 0.01–100 mW cm^{-2}.[64–66] In a study performed by Luu *et al.*, using (2,4,6-trimethylbenzoyl)phosphine oxide (BAPO) as a photoinitiator, the effect of UV light intensity on photopolymerisation of 2-hydroxyethyl methacrylate (HEMA) was evaluated, and Raman spectroscopy quantified the conversion yield (degree of crosslinking) and polymerisation rate. The range of UV light intensity (0.01–3 mW cm^{-2}) was studied to see the effect of free-radical polymerisation and chain termination pathways. The degree of crosslinking was the same with all the light intensities from 0.01–3 mW cm^{-2}, but the polymerization rate was higher with 1–3 mW cm^{-2} light intensity (0.030 s^{-1}) that reduced significantly with light intensities lower than 0.1 mW cm^{-2} (0.015–0.01 s^{-1}).[66] In another study by

He *et al.*, they formulated a photopolymerisable hydrogel using poly(methacrylic acid) (PMAA) crosslinked with tri (ethylene glycol) methacrylate (TEGMA) in an Irgacure 651 – based free radical photopolymerisation technique. The effect of different ranges of UV light intensity (2–24 mW cm^{-2}) on the photopolymerisation reaction kinetics of the gel as well as physical and rheological properties, were studied. The hydrogel crosslinked with higher-intensity UV light showed faster polymerisation kinetics and a higher swelling ratio. However, the gel conversion percentage significantly decreased (99% to 61%) from lower to higher light intensity due to faster chain termination with higher-intensity light. Higher light intensity results in a faster and higher generation of free radicals, leading to intramolecular cyclisation that forms microparticle islands rather than macrogels. With low light intensity, fewer free radicals are generated, leading to lower reaction kinetics, which results in the formation of macrogel rather than microgels clusters and a higher macrogel conversion rate. The degree of macrogel formation is higher with low light intensity than with high light intensity, which forms microgels.[67] In another study by O'Connell *et al.*, GelMA hydrogel photopolymerization was done using Irgacure 2959 photoinitiator at 0.5% w/v concentration with different light intensities ranging from 2–150 mW cm^{-2}. The generation of free radicals was dependent on the light intensity, with the highest number of free radical generation at 150 mW cm^{-2} (7.0×10^{18} free radicals) and the lowest number of free radical generation at 2 mW cm^{-2}. Similarly, the GelMA crosslinking rate increased with higher intensity light 150 mW cm^{-2} having peak crosslinking at 20 seconds, whereas lower intensity light 2 mW cm^{-2} had a peak crosslinking at 100 seconds.[36]

For the development of a 3D tissue model, it is essential to optimise all the factors mentioned, as each has a negative effect on cell viability with increased levels. With increased photoinitiator concentration and UV intensity, a large influx of free radicals takes place, impacting cell viability negatively. In a study by Shie *et al.*, cell proliferation decreased with increasing concentrations of GelMA (5%, 10% and 15% w/v) due to lower cell adhesion with the substrate.[68] Similarly, a study by Wu *et al.* depicted that the cell spreading is also hampered due to the gel's stiffness, which does not allow the actin and myosin filaments to configure freely through the matrix.[69] Hence, achieving an optimal concentration of all three factors is essential to develop various tissue constructs. The optimal concentration of GelMA and other parameters will aid the growth and development of 3D tissue models.

2. Synthesis of GelMA

GelMA fabrication was first described by Van Den Bulcke *et al.*, which is considered the conventional method for GelMA synthesis. Briefly, methacrylic anhydride (MA) is reacted with gelatin amino groups, resulting in grafting of MA methacryloyl groups (methacrylamide, methacrylate groups) on gelatin amino groups (lysine and hydroxyl lysine) forming methacrylamide modified gelatin/gelatin methacrylate. The conventional method of GelMA synthesis is a two-step process. Gelatin is

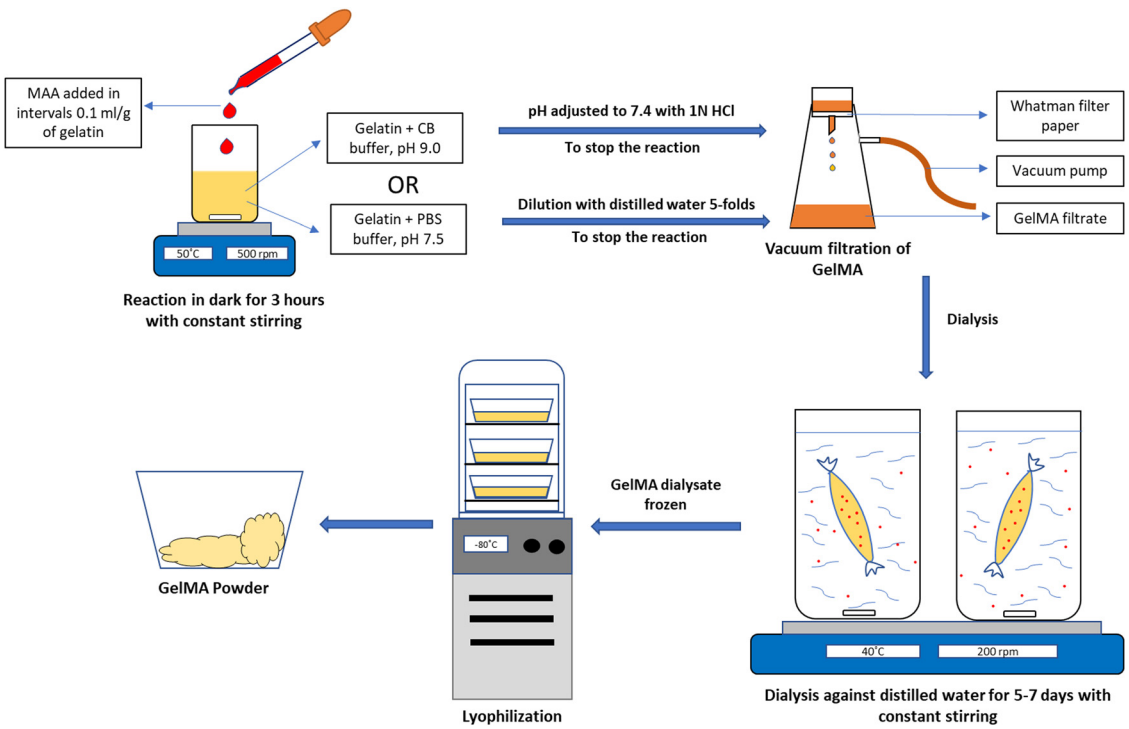

Fig. 4 Schematic representation of GelMA synthesis using Carbonate-Bicarbonate buffer (CB buffer) or Phosphate Buffer Saline (PBS).

dissolved in phosphate buffer saline (pH 7.5) at 50 °C, and MA is added to the gelatin solution. After 1 hour of reaction, the mixed solution is diluted 5 folds to stop the reaction. The mixture is dialysed against distilled water at 40 °C for 5 to 7 days to remove unreacted MA and lyophilised to obtain GelMA in powder form. GelMA hydrogel is prepared in the subsequent step by UV photocrosslinking of derivatised gelatin in the presence of a photoinitiator. Irgacure 2959 and LAP are the two commonly used water-soluble photoinitiators. Irgacure 2959 can be initiated from 276 nm to a maximum of 365 nm, whereas LAP gets initiated at 370–405 nm.[70] Studies have reported that LAP is more suitable for biological applications due to the low initiation frequency and crosslinking time, making it lower cell toxicity.[24] Fig. 4 depicts the method and steps for synthesizing GelMA polymer.

2.1 Buffer system

The degree of substitution (DS) is a significant parameter for controlling all the properties of GelMA, including its mechanical properties. The GelMA DS is a function of gelatin and methacrylic anhydride (MA) concentration used. Hydrogel with specific DS can be obtained by fine-tuning the gelatin : MA ratio.[71,72] Studies have been carried out to develop methods for synthesising GelMA with high DS. The conventional method of GelMA synthesis using PBS (pH 7.4) as solvent requires a higher MA concentration to obtain GelMA with high DS. The use of high MA concentration may lead to toxicity of cells if MA is not completely eliminated during the dialysis process. Several studies have been carried out to study the effect of different buffer systems on GelMA DS. Lee *et al.* investigated the effect of different buffer, pH and MA concentrations on GelMA DS. They synthesised GelMA in both PBS (pH 7.8) and carbonate bicarbonate buffer (CB buffer pH 9). GelMA synthesised by sequential addition of MA in PBS and CB buffer resulted in a drop in pH below the isoelectric point (IEP) 7–9 of type A gelatin. For maintaining the pH of the reaction mixture above the IEP of gelatin, they proposed a new sequential MA addition method by readjusting the pH of the gelatin solution to the optimal pH of the buffer system every 30 minutes. By sequential addition of MA with pH adjustment, they were able to produce GelMA with DS of 80% and 97% in PBS and CB systems. The study also indicates the effect of MA concentration on the DS of GelMA. GelMA in PBS requires a higher MA feed ratio (0.6 ml–2 ml g^{-1} of gelatin) to obtain DS of around 80–90%, whereas GelMA prepared in CB buffer with an MA feed ratio of 0.1 ml g^{-1} of gelatin resulted in nearly 100% DS. The proposed method is efficient in synthesising GelMA with high DS by significantly decreasing the MA molar ratio to 2.2-folds from 10–32 folds for the conventional method using PBS. This enables specific control of mechanical properties to obtain soft and stiff hydrogel using GelMA with different degrees of substitution.[73] In another study, Lee *et al.* synthesised GelMA using both type A and type B gelatin in CB buffer by following the same method. They studied the mechanical properties and printability of GelMA hydrogel for 3D bioprinting applications. GelMA hydrogel was prepared by UV crosslinking with Irgacure 2959 as the photoinitiator. GelMA produced using type B gelatin resulted in the highest DS at a lower MA feed ratio of 0.1 mg g^{-1} of gelatin compared to type A gelatin. The higher DS of type B GelMA is attributed to many free amino groups reacting with MA at pH 9, which results in a higher degree of substitution. In their study, type A and type B GelMA at 20% w/v concentration showed good shear thinning properties.[74] The major drawback with GelMA synthesis by sequential MA addition is that it requires physical pH adjustment before each MA addition, which is laborious. To overcome this issue, Shirahama *et al.* proposed a facile one-pot method for GelMA synthesis, which requires only initial pH adjustment. The study was based on the inference from their previous study that CB buffer with a pH adjustment of pH 9 enables the synthesis of GelMA with higher DS ($\geq$97%) as compared to the conventional method using PBS. They also studied the effect of different reaction parameters, such as molarity and pH of CB buffer, for the controlled synthesis of GelMA. Using 0.25 M CB buffer with an initial pH adjustment of pH 9, which is higher than the IEP of type A gelatin, resulted in the synthesis of GelMA with nearly complete DS ($\geq$95%).[75]

2.2 Determination of degree of substitution (DS) or degree of functionalization (DoF)

The degree of substitution (DS) of GelMA hydrogels directly affects the GelMA physical properties such as porosity, swelling and degradation, and mechanical stiffness. The general DS of GelMA ranges from 30–100%.[21,71,76,77] The degree of substitution (DS) of the synthesised GelMA is determined by ^{1}H NMR method by spectral peak integration corresponding to the methacrylic functional group and compared with unmodified gelatin and calculated as the moles of the methacrylic group per gram of proteins.[78] One drawback of quantifying DS with ^{1}H NMR technique is that the precise amine content in the GelMA should be known. Hence, along with ^{1}H NMR technique, researchers have also performed a colourimetric method for quantifying amine content in GelMA hydrogel. Shirahama *et al.* used 2,4,6-trinitrobenzene-sulfonic acid (TNBS) assay to determine DS in GelMA prepared in different buffer systems and gelatin concentration and the amino group concentration were determined by plotting a standard glycine curve.[75] Zatorski *et al.*, reported another colorimetric assay known as the Ninhydrin assay for the quantification of DS in GelMA hydrogel. The Ninhydrin assay is used to determine the free amine group present in a solution after the conjugation reaction, and the DS is calculated by subtracting the fraction of unreacted amine groups available in the solution after the methacrylation reaction. The fraction of the unreacted amine group is determined from a standard calibration curve prepared from dissolving unmodified gelatin in PBS at different concentrations (0–10 mg ml^{-1}). The colourimetric study was done by adding Ninhydrin solution (2.2 mg ml^{-1}) to the samples in a ratio of 1 : 8 v/v and incubating at 70 °C for 20–30 minutes, after which the absorbance was measured at 570 nm.[79]

3. Properties and application of GelMA in tissue engineering

The properties of GelMA hydrogel, such as viscosity, porosity, degradation, swelling, mechanical and rheological properties, are significant factors determining the fabrication and viability of tissue constructs.

3.1 Viscosity

The printability of GelMA hydrogel is influenced by the viscosity of hydrogel and shear thinning properties that affect the bioprinted construct's structural fidelity. The optimum viscosity for bioprinting GelMA could be achieved by varying factors such as polymer concentration, the temperature of GelMA, and adjusting the degree of photocrosslinking.[80] For the printability of GelMA hydrogels, the optimal viscosities of the bioink should range from 100–1000 Pa s for proper extrusion of the bioink.[25,27] In a study by Yin *et al.*, a two-step crosslinking strategy was developed for 3D Bioprinting of GelMA hydrogel. The bioink was prepared with a combination of GelMA and gelatin with 5% and 8% w/v, respectively. In the first step, thermally reversible gelatin crosslinking was employed to obtain a bioprinted construct with high fidelity. In the next step, irreversible photocrosslinking of GelMA was utilised to get the bioprinted construct. The GelMA/gelatin bioprinted construct showed 90% cell viability when printed with bone marrow stem cell (BMSCs) laden GelMA/Gelatin bioink.[25] Embedded printing is another way to obtain a high-fidelity structure besides using composite GelMA bioink formulation for the 3D bioprinting process. In a study by Ning *et al.*, GelMA hydrogels were printed within a Carbopol suspension bath to fabricate a high-fidelity 3D bioprinted structure. The Carbopol suspension bath system maintained the structural architecture of the bioprinted GelMA construct and the construct was easily extracted after PBS wash. Human Umbilical Vein Endothelial cells (HUVECs) laden GelMA bioink was printed with and without a Carbopol suspension bath. The biocompatibility study showed higher cell viability and metabolic activity with constructs printed within the Carbopol bath.[81] Although GelMA bioink exhibits shear-thinning properties, if GelMA bioink is too viscous, it may clog the nozzle during printing and if it is too thin, then the 3D printed structural fidelity is compromised. Hence, researchers have tried blending GelMA hydrogel with other biomaterials to achieve optimal rheological properties for bioprinting.

3.2 Porosity and pore size

The hydrogel porosity of 3D tissue constructs is essential in determining tissue architecture by cellular distribution and cell penetration through the matrix. Increased porosity within the hydrogel scaffold can also help in nutrient and oxygen diffusion without vascular networks. Thus, a tissue construct's porosity significantly impacts cell survivability, proliferation and migratory pattern.[82] The pore size of the GelMA matrix may range from a microporous pore ranging from 50–100 μm to macropores ranging from 200–700 μm.[83–85] In a study by Song *et al.*, a GelMA – micro/nano hydroxyapatite (HAp) composite hydrogel scaffold was 3D printed using digital light processing (DLP) to form a porous matrix for bone tissue regeneration. The scaffold's porosity was adjusted by altering the GelMA concentration, degree of GelMA substitution and addition of either micro/nano – HAp. *In vitro* biocompatibility studies of the 3D printed scaffold showed good cell adhesion, proliferation of osteoblast cells and osteogenic differentiation. *In an in vivo* animal model using rabbits, the cellular 3D-printed scaffold showed new bone formation in critical bone defects in the skull.[86] In a study done by Usal *et al.*, GelMA-poly(2-hydroxyethyl methacrylate) (pHEMA) hydrogel was prepared at 15% w/v GelMA combined with pHEMA at different v/v ratio (9 : 1, 8 : 2, 7 : 3, 6 : 4 and 5 : 5). The porosity of the hydrogel was analyzed using SEM imaging and in 15% w/v GelMA had the highest porosity of 70% and an average pore size 40 μm. The porosity of pHEMA was 15%, and the pore size was 15 μm, while the combination of GelMA-pHEMA from 9 : 1 to 5 : 5 v/v had a porosity of 20–65% and pore size ranging from 15–40 μm. Schwann cell proliferation was studied in GelMA, pHEMA and GelMA-pHEMA (5 : 5 v/v) hydrogel using Alamar Blue assay, which showed the best result with GelMA-pHEMA (5 : 5 v/v) matrix and least cell proliferation with pHEMA matrix.[87] In another study performed by Yang *et al.*, a 3D printed antibacterial wound dressing was fabricated using GelMA and Xanthan gum composite hydrogel with the incorporation of *N*-halamine – TiO_2 nanoparticles providing the antibacterial properties of the wound dressing. The GelMA concentration was fixed at 15% w/v, and the xanthan gum concentration varied (0%, 1%, 2% & 3% w/v) to formulate the bioink. The 3D printed dressing showed an increase in printing fidelity with the increase in the concentration of xanthan gum, whereas the porosity of the structure was decreased minimally with an increase in xanthan gum concentration with small microporous structures seen on pore walls, which increased at higher xanthan gum concentration.[88] Porosity in GelMA hydrogel plays an essential role in understanding cell infiltration and distribution that facilitates tissue development and regeneration. The above studies show that porosity influences cell proliferation by providing space for cells to grow and divide. Pores ensure enough oxygen and nutrient diffusion to maintain cell viability and can also influence cell differentiation. GelMA porosity can be varied by changing the GelMA concentration or blending with other polymers.

3.3 Swelling & degradation

Hydrogels are polymeric materials that can uptake water when placed in an aqueous environment and retain them within their lattice structure through hydrophilic interaction. The uptake of water molecules results in swelling until an equilibrium is reached. Further, swelling can occur after equilibrium by degradation-induced swelling. The hydrogel network loses its elastic restorative force, leading to further swelling up of hydrogel, followed by bulk degradation and disintegration of the hydrogels. Hence, precise control over the swelling and degradation kinetics is essential to fabricate hydrogels that

would meet the needs of biomedical applications.[89] The swelling percentage of GelMA may range from 600–1000% of its initial dry weight.[27,90] Depending on the degree of crosslinking, the *in vitro* degradation of GelMA hydrogels in collagenase type II solution at a concentration of 1–20 U ml^{-1} is more than 50% within 0.5–3 hours.[91–93] In a study done by Kim *et al.*, a nanostructured vascular pattern was fabricated using a combination of Polyethylene glycol diacrylate (PEGDA – 5% & 20% w/v) and different concentrations of GelMA (5%, 10% & 20% w/v) hydrogel by capillary force lithographic technique. The degradation kinetics of PEGDA-GelMA hydrogel was determined by placing hydrogels in collagenase II solution and determining the degradation percentage after 1, 3 and 7 days. The result showed an exponential degradation pattern during the initial degradation phase. The degradation kinetics with 5% w/v PEGDA and 20% w/v GelMA showed greater than 60% mass loss at day 7 whereas with 20% w/v PEGDA and 5% w/v GelMA, the mass loss was only 20% after day 7. The hydrogel matrix stiffness with 20% w/v PEGDA and 5% w/v GelMA concentration was 0.88 ± 0.06 MPa, which was similar to that of 5% w/v PEGDA and 20% w/v GelMA concentration (0.87 ± 0.06 MPa). Hence, even with the similar stiffness with the two different combinations of PEGDA and GelMA concentration, the degradation with higher GelMA was still faster due to the activity of collagenase compared to PEGDA.[94] In another study performed by Bittner *et al.*, the GelMA-Gelatin microparticle (GMP) composite hydrogel construct was 3D printed, and its swelling and degradation properties were evaluated over a period of time. The gelatin microparticles were crosslinked using 10 mM glutaraldehyde (GMP-10) or 40 mM glutaraldehyde (GMP-40). The composite bioink was prepared by dispersing GMP-10 and GMP-40 in 5% w/v GelMA solution and stored in the refrigerator before printing. The swelling properties of the GelMA construct and GelMA/GMP composite construct were evaluated for up to 28 days. The GelMA/GMP-10 construct showed a higher swelling ratio than the GelMA-only construct, whereas GelMA/GMP-40 showed a lower swelling ratio than the GelMA-only constructs; further, with the inclusion of GMPs in GelMA hydrogel, significant polymer loss was observed up to day 21.[95] The swelling and degradation properties can be controlled by varying the concentration of GelMA and also by blending with other polymers. The swelling and degradation profile of GelMA hydrogels can be tuned for optimum tissue regeneration.

3.4 Mechanical and rheological properties

The rheological properties of hydrogels are an essential characteristic that determines the printability of the 3D tissue construct. GelMA is a chemically modified gelatin polymer product that has the unique property of undergoing reversible thermal gelation. The sol–gel transition occurs when the GelMA solution is cooled, resulting in physical crosslinking forming helical-like polymer conformation. This provides the GelMA with adequate viscosity for the 3D bioprinting application. The covalent crosslinking of the methacrylic group determines the mechanical strength of GelMA *via* photopolymerisation, which supports 3D construct development for tissue engineering applications.[96] Although GelMA shows better mechanical strength than other naturally derived polymers, its mechanical strength is still low compared to synthetic hydrogels. Hence, researchers have focused on copolymer GelMA systems for developing hydrogels with appropriate mechanical strength for tissue engineering applications.[97] The storage modulus of GelMA hydrogel to support cell-based assay ranges from 0.1–30 kPa.[21,27,93,98] In the study by Joseph *et al.*, a T-cell activation study was performed by fabricating a 3D matrix of different stiffness with cell-laden GelMA hydrogel using digital light processing (DLP) based 3D bioprinting technique with photopolymerisation at 405 nm. Mouse lymphoma T-cell line (EL4) or primary mouse T-cell was used to fabricate the 3D cell-laden GelMA construct with the addition of 10 ng mL^{-1} of phorbol myristate acetate (PMA) and 0.1 μM of ionomycin to check for the activation of T-cell. Two different concentrations of GelMA (10% w/v and 15% w/v) were used to provide the matrix stiffness (19.83 ± 2.36 kPa and 52.95 ± 1.36 kPa) for maintaining a physiologically relevant lymph node condition. Thirty-six hours post-activation of T-cells, the cell viability and IL-2 release by activated and non-activated T-cells was quantified, which showed that there was no significant increase of cell viability from the activated and un-activated cells (84.89% and 89.5% viability in 10% w/v GelMA matrix) but there was a significant release in IL-2 for activated T-cells compared to un-activated ones and the release of IL-2 in 3D bioprinted matrix was 7.4-folds and 5.9-folds higher for 10% w/v and 15% w/v GelMA respectively compared to 2D culture.[99] In another study by Wang *et al.*, a copolymer hydrogel was prepared using dextran glycidyl methacrylate (DexMA) and GelMA hydrogels to develop an extracellular matrix scaffold. The hydrogel's mechanical properties were increased by increasing the degree of substitution (DS) of DexMA hydrogel when prepared with a constant GelMA concentration. Higher compressive modulus was reported with the copolymer of GelMA and high DS DexMA compared to GelMA hydrogel alone. The cell viability at day 1 was higher in GelMA (88.35%) compared to GelMA-DexMA (56.91%), which increased to 72.65% on day 6 for GelMA-DexMA.[100] Table 3. Summarise GelMA hydrogel prepared with different gelatin types, buffer systems and methacrylic anhydride concentrations and their properties.

Several studies using GelMA in different tissue engineering applications have shown good biocompatibility and cell viability. However, their application in tissue engineering, such as cartilage repair, is limited due to their poor mechanical property. Also, it has been reported that the mechanical properties and structural fidelity of GelMA hydrogels can be improved by increasing polymer concentrations (>15% w/v), but this would adversely affect the hydrogel's cell viability, porosity and other properties. Several other biomaterials have been incorporated with GelMA to form biohybrid/composite materials to improve their mechanical properties.[19] A range of natural and synthetic polymers such as hyaluronic acid, alginate, chitosan, poly(ethylene glycol) (PEG), poly(acrylic acid) (PAA), and other inorganic materials such as carbon nanotubes (CNT), graphene oxide (GO) are commonly used for combining with GelMA for

Table 3 Summary of GelMA hydrogel parameters for different tissue engineering applications

Gelatin type	Gelatin concentration	Buffer system	MA concentration(per g of gelatin)	DS.%	Properties			Ref.
					Mechanical	Physical	Biological	
Type B 250 bloom	10% w/v	CB (0.25 M)	0.9 ml	100%	Storage modulus 30.20 ± 0.57 kPa	Degradation in collagenase 50% mass loss: 3.23 hours	Huh7.5 cells cell viability More than 87%	93
				60%	Storage modulus 16.04 ± 0.93 kPa	Degradation in collagenase 50% mass loss: 0.65 hours	Huh7.5 cells cell viability More than 87%	
Type A 300 bloom	10% w/v	CB (0.25 M)	0.2 ml	100%	Storage modulus 444.5–1640 Pa	Degradation in collagenase 20–30% mass loss: 3 h	hAD-MSCs cell viability after day 7 90–100%	21
			0.025 ml	70%	Storage modulus 174–214.5 Pa	Degradation in collagenase 50–70% mass loss: 3 h	hAD-MSCs cell viability after day 7 90–100%	
Type A 250 bloom	10% w/v	PBS	0.5 mL min^{-1}	96%	Young's modulus 2.08 ± 0.43 kPa (5% w/v GelMA) 264.74 ± 11.08 kPa (30% w/v GelMA)	Swelling ratio in PBS 44.57 ± 3.05 (5% w/v GelMA) 4.05 ± 1.19 (30% w/v GelMA)	BMSCs viability after day 7 Higher than 90% (5% w/v GelMA) 70.4 ± 0.44% (30% w/v GelMA)	25
Type A 300 bloom	10% w/v	PBS	0.2 ml	52.5%	Young's modulus	Degradation in collagenase	HCC1806 cell viability	91
						63.4% (UV crosslinked) mass loss: 1 h	86.7% ± 2.1% (UV crosslinked)	
					3562.4–3124.8 Pa	27% (UV + mTG crosslinked) mass loss: 1 h	85.7% ± 4.1% (UV + mTG crosslinked)	
Type A	10% w/v	PBS	2 ml	89%	Compressive modulus 5.8 kPa (10% GelMA)	Degradation in collagenase 100% degradation at day 1 (10–20 U ml^{-1})	HCEC cell density Lower than 1500 cells per mm^2 (unpatterned GelMA)	92
					56.7 kPa (30% w/v GelMA)	55% degradation at day 7 (1 U ml^{-1})	1500–2000 cells per mm^2 (patterened GelMA)	
Type A 300 bloom	10% w/v	PBS	0.6 ml	87–90%	Storage modulus 0.1–1 kPa	Swelling percentage in PBS 800–1000%	NIH3T3 cell viability More than 100% (day 14)	27
Type A 300 bloom	10% w/v	PBS	0.74 ml	82 ± 5%	Storage modulus 1–3 kPa	Degradation in PBS 40–70% mass loss: 30 days	C2C12 myoblasts cell viability More than 90% (day 3)	98

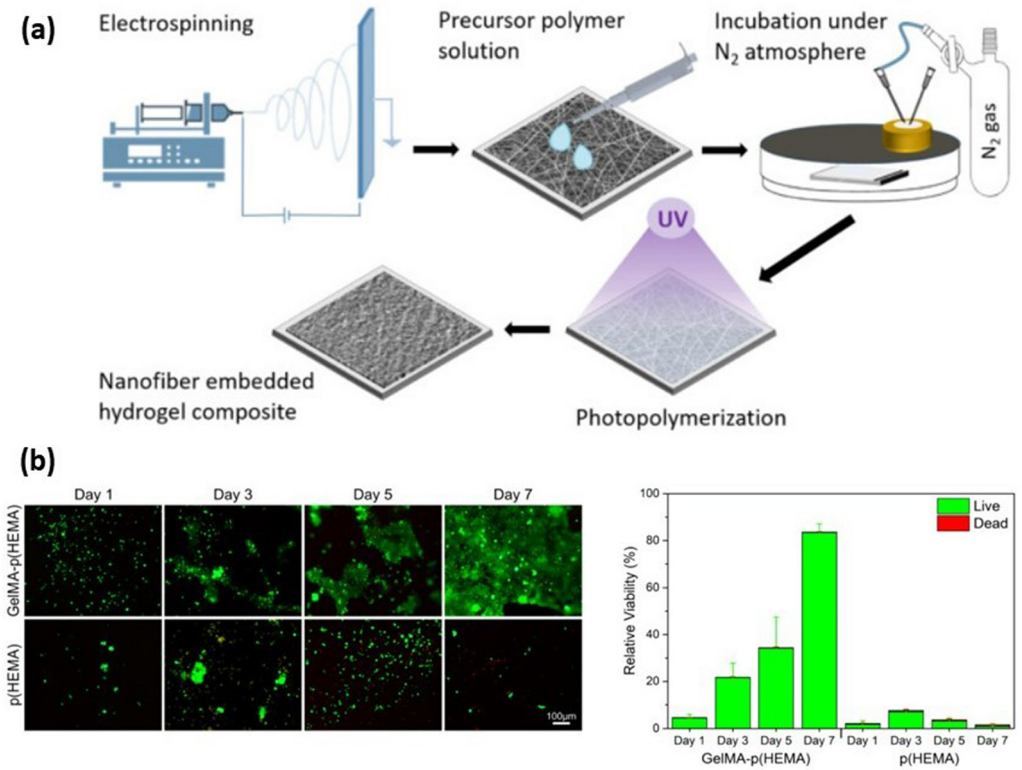

Fig. 5 (a) Fabrication of composite hydrogels using electrospun Gelatin Methacryloyl (GelMA) fibres embedded in a poly(2-hydroxymethyl methacrylate) p(HEMA) matrix. (b) Biocompatibility of p(HEMA) and GelMA-p(HEMA) hydrogels analysed using live/dead staining (qualitative) and Alamar Blue assay (quantitative). Reproduced from ref. 103 with permission from Elsevier, copyright (2021).

enhancing their mechanical properties.[101] For the treatment of anterior lamellar keratoplasty, Arica *et al.*, prepared GelMA composite hydrogels with the addition of poly(2-hydroxyethyl methacrylate) (p-HEMA) polymer. GelMA at concentrations of 3%, 5% and 10% w/v were prepared and electrospuned (Fig. 5a) into fibres, and pHEMA prepolymer at 10% w/v concentration was polymerized with and without GelMA fibres. In the presence of GelMA, higher protein absorption of human serum albumin (HAS), Immunoglobulin (IgG) and lysozyme (LYZ) was seen compared to pHEMA hydrogel. Higher cell viability was observed with GelMA-pHEMA compared to pHEMA hydrogel (Fig. 5b)[102]. In another study by Wang *et al.*, GelMA-pectin methacrylate (PECMA) composite hydrogel was prepared for hemostatic effect and cell viability with encapsulated L929 fibroblast cells was studied. PECMA hydrogel was combined with GelMA crosslinked with Ca^{2+} ion to develop an interpenetrating hydrogel network that can be injected at the wound site and then UV photopolymerized (Fig. 6a). Slower blood coagulation time with GelMA/PECMA hydrogel without Ca^{2+} (9 min 45 s) compared to GelMA/PECMA hydrogel with Ca^{2+} crosslinking (6–7 min) (Fig. 6b and c)[103]. The tuneable mechanical and adhesive properties of the GelMA hydrogel were shown by Tavafoghi *et al.*, where GelMA and alginate methacrylate (AlgMA) composite hydrogel were prepared. The Young's modulus of the blended hydrogel increased threefold compared to pure GelMA hydrogel. The wound closure strength and adhesion energy were 1.5–2.5 folds more compared to pure GelMA (Fig. 7a). The cell viability was similar with or without the addition of AlgMA, but metabolic activity increased with increased concentration of AlgMA (Fig. 7b.)[104]. Table 4 summarises different composite GelMA hydrogels used for tissue engineering applications and their properties.

4. Applications of gelma in 3D bioprinting

The demand for tissues and organs for transplantation has seen significant growth due to the limited number of donors and the presence of viable tissues. The significant limitations associated with current approaches for organ impairment, such as autograft and allograft transplantation, are donor shortage, high cost, secondary trauma, and immune rejection.[108] Over the past three decades, tissue engineering has emerged as a promising alternative technique to tackle the shortage of donors. The conventional approach in tissue engineering for organ and tissue repair or regeneration is based on cell-seeded porous scaffolds. The major problem associated with the conventional approach is heterogeneous cell distribution and poor vascularisation, which hinders their application in the regeneration of highly complex tissues.[109] To address the

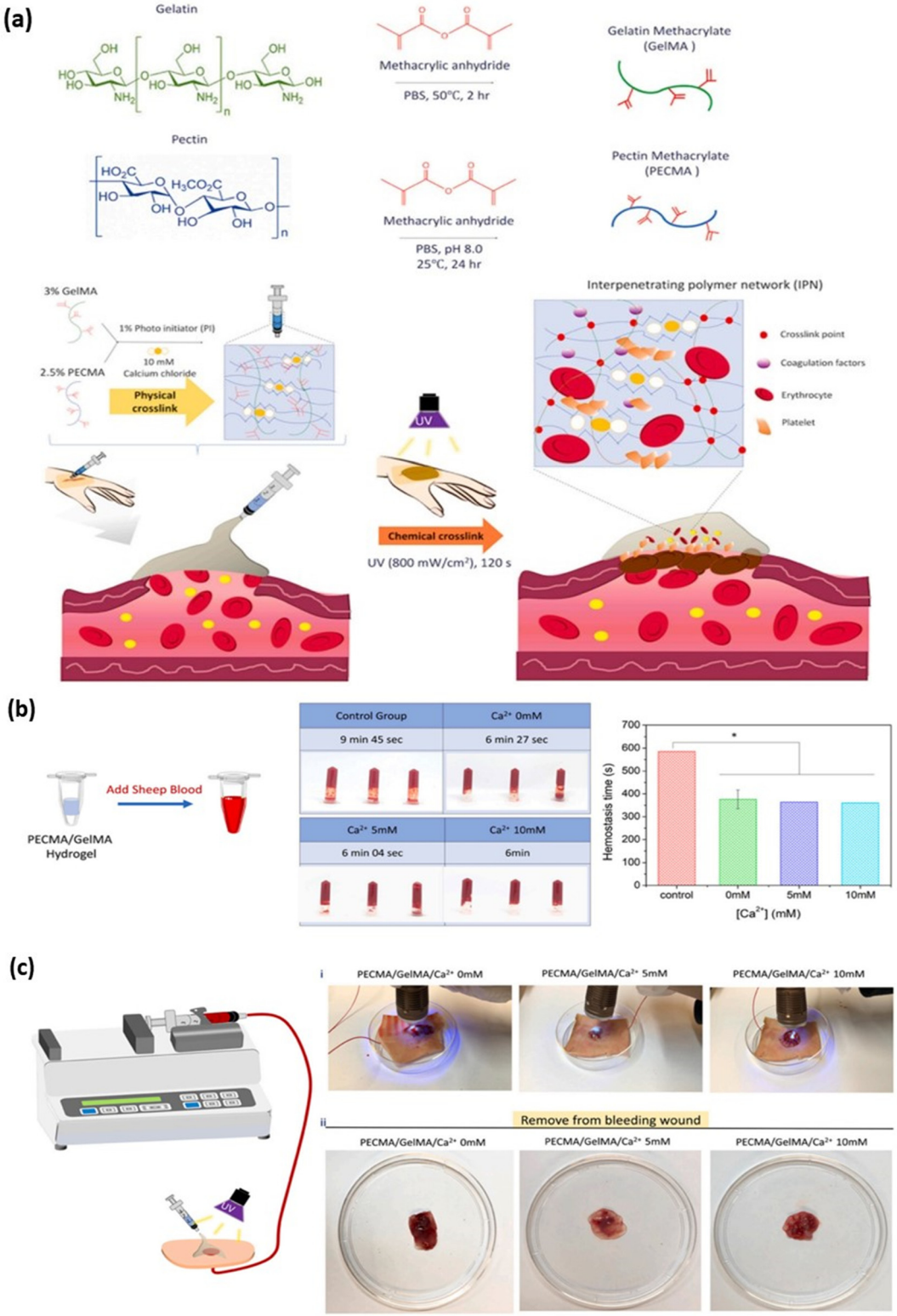

Fig. 6 Development of a hybrid dual crosslinked pectin methacrylate (PECMA) – gelatin methacrylate (GelMA) hydrogel for hemostatic application. (a) Schematic representation of PECMA/GelMA hydrogel and its dual crosslinking mechanism forming an interpenetrating network (IPN) for application in skin hemostasis. (b) Hemostatic effect of PECMA/GelMA hydrogel on sheep blood in the presence of different concentrations of calcium ion (0, 5 & 10 mM) as test group and without hydrogel as control group (c) images representing the *in vitro* porcine skin bleeding model with PECMA/GelMA hydrogel injected onto the wound site for blood coagulation and extent of coagulation at different concentration of calcium ions (0, 5 & 10 mM). Reproduced from ref. 103 with permission from Elsevier, copyright (2021).

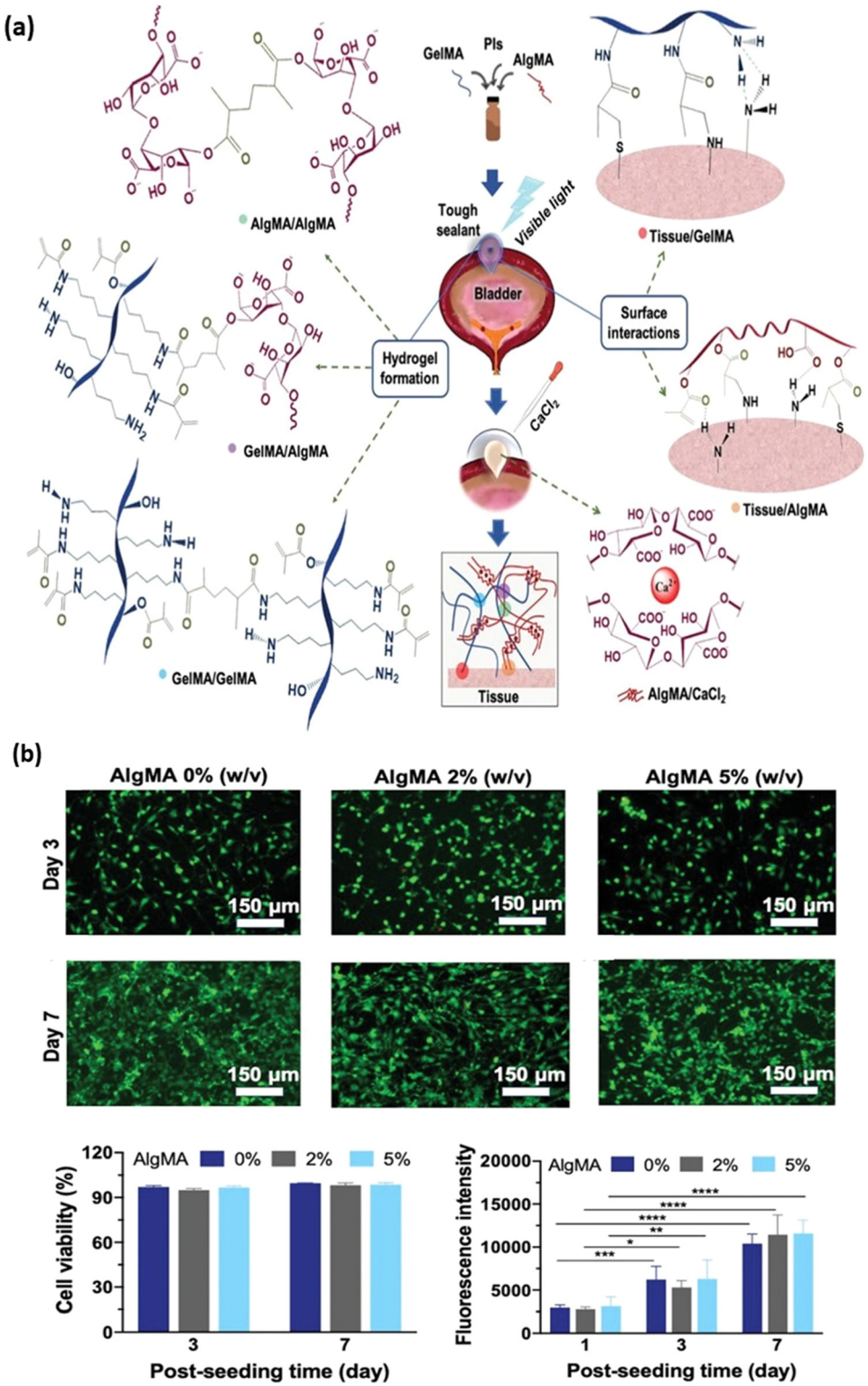

Fig. 7 Development of a hybrid composite hydrogel consisting of gelatin methacryloyl (GelMA) and alginate methacrylate (AlgMA) as a bioadhesive. (a) Schematic representation of covalent crosslinking of GelMA-AlgMA composite hydrogel *via* photopolymerisation of methacrylate group and ionic crosslinking between alginate group. The hydrogel and the tissue surface bonding interaction is depicted. (b) Cytotoxicity study of the hydrogel composed of 20% w/v GelMA with varying concentrations of AlgMA is observed using life/dead staining, and metabolic activity quantified using PrestoBlue reagent (Invitrogen). Reproduced from ref. 104 with permission from John Wiley and Sons, copyright (2020).

Table 4 GelMA-based composite hydrogels and their properties

Components	Properties	Cell type	Ref
GelMA/poly-acrylamide (PAM)	• Better thermal stability at 32–34 °C (storage modulus >1000 Pa) compared to gelatin hydrogel (storage modulus < 400 Pa) • Higher viscoelasticity (0.48 MPa) at 60% compression compared to GelMA (0.2 MPa) • The pore size of pure GelMA hydrogel was 100 μm, and pure PAM hydrogel was 20 μm. For GelMA/PAM hydrogel, an increase in PAM concentration results in small pore size • GelMA and GelMA/PAM hydrogel had lower swelling ratio compared to PAM hydrogel, slower degradation (70% degradation on day 17) compared to GelMA hydrogel (100% degradation on day 8)	Chondrocytes	105
GelMA/poly(2-hydroxyethyl methacrylate) (p-HEMA)	• A notable improvement in tensile strength (approx. 500 kPa) compared to GelMA (360 ± 40 kPa) • Young's modulus (7 ± 1 kPa) is slightly lower than human corneal modulus (100–5700 kPa) • Better haemolytic activity (4.57 ± 0.09%) compared to p-HEMA (1.63 ± 0.04%) • Higher cell viability (>80%) compared to p-HEMA (<10%) at day 7	Corneal endothelial cells	102
GelMA/pectin methacrylate (PECMA)	• The swelling ratio was higher with PECMA concentration at 2.5% w/v than 1.5% w/v in GelMA/PECMA hydrogel • The compressive modulus of PECMA – GelMA (2.5 : 3% w/v) increases with increased calcium concentration from 0–10 mM Ca^{2+} concentration • Slower blood coagulation time with GelMA/PECMA hydrogel without Ca^{2+} (9 min 45 s) compared to GelMA/PECMA hydrogel with Ca^{2+} crosslinking (6–7 min)	L929	103
GelMA/alginate	• Polymer concentrations at GelMA–alginate (6%: 7% w/v) had a swelling ratio of 2.5 compared to GelMA–alginate (6%: 5% w/v) having a swelling ratio of 1.7 • Improved storage modulus with G6A7 (45.3 ± 3.5 kPa) compared to G6A7 (31.7 ± 1.2 kPa) • 86% cell viability in G6A7 hydrogel compared to 80% cell viability with G6A5 hydrogel	Sheep adipose-derived stem cells (sADSCs)	106
GelMA/alginate methacrylate (AlgMA)	• The addition of AlgMA concentration from 2–3% w/v increases the young's modulus by 3-fold over GelMA hydrogel • 3% w/v AlgMA concentration has a swelling ratio of 20% compared to AlgMA-free hydrogel, which has a swelling ratio of 5% • The collagenase degradation of hydrogel without AlgMA is 90% compared to hydrogel with 4–5% w/v AlgMA having a degradation of 40%	NIH-3T3 fibroblast cell	104
GelMA/carbon nanotube (CNT)	• Higher mechanical properties of GelMA/CNT hydrogel (24.2 ± 0.2 and 30.6 ± 0.7 kPa for random and aligned oriented CNT) compared to pristine GelMA (15.8 ± 0.4 kPa) • Electrical conductivity increases from 0 mA in pristine GelMA to 24.2×10^{-7} mA with GelMA/CNT aligned orientation • Tnnt2 cardiac gene expression level in the embryonic body was 3.24 ± 0.50 for pristine GelMA and 10.17 ± 3.39 in GelMA/CNT aligned with electrical stimulation	129/SVE-derived mouse stem cells	107

shortcomings of conventional methods, bio-fabrication-based methods like 3D bioprinting have gained enormous interest worldwide.

3D bioprinting is derived from the concept of additive manufacturing and works based on the layer-by-layer manufacturing process. This technology helps in the fabrication of tissues or organs by progressive layer-by-layer addition of cell-laden hydrogels (bioinks) into predefined 3D models designed using computer-aided design (CAD).[110] The major challenge of 3D bioprinting is the development of suitable bioinks with optimal structural fidelity mechanical and physical properties that resemble biological tissues. Among the biomaterials used as bioink, GelMA has recently gained massive attention. GelMA satisfies the requirements of an ideal bioink, such as mechanical tunability, high structural fidelity, printability, excellent biocompatibility and biodegradability.[101] The number of publications in the last 5 years for fabrication of various tissue construct using GelMA based 3D bioprinting approach is illustrated in (Fig. 8) which is compiled from Scopus database using keywords like GelMA, 3D bioprinting and specific tissues.

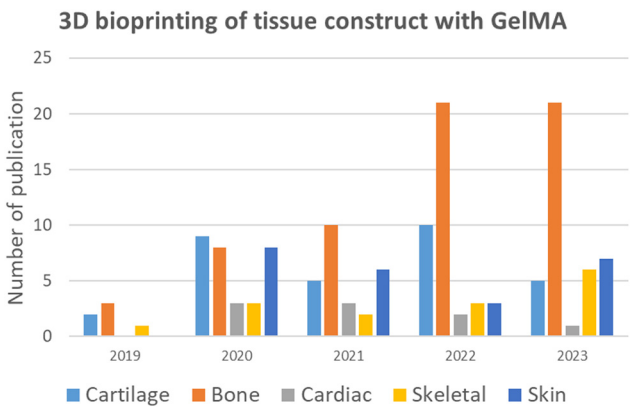

Fig. 8 Number of publications of various tissue constructs with GelMA hydrogel in the last 5 years using the 3D bioprinting approach.

4.1. Cartilage

Cartilages are dense connective tissues primarily composed of chondrocyte cells distributed in an extracellular matrix of proteoglycans, collagen and glycosaminoglycan (GAG).[111] There are 3 major cartilages in the human body; the most predominantly present cartilage is the hyaline articular cartilage. Hyaline cartilage comprises chondrocytes, GAG, collagen type II and proteoglycan, found in the synovial joints, protecting bones from abrasion and for smooth joint movement.[112] Fibrocartilages are found in temporomandibular joints, the joint meniscus and the annulus fibrous of intervertebral discs and are mainly composed of collagen type I and chondrocytes.[113] Elastic cartilages are yellowish in colour and are found in the external ear, larynx and epiglottis. The extracellular matrix of elastic cartilage is made up of collagen type II, proteoglycan and elastin fibres, which give the yellowish colour.[114] Cartilage degeneration can occur due to articular or fibrocartilage injury, leading to arthritis. The surgical-based approach to treatment isn't always able to repair cartilage defects, and a wide range of tissue engineering approaches is currently under development to overcome the limitation of cartilage autografts.[115] The mechanical, swelling and hydration properties of GelMA hydrogel are similar to native cartilage tissue.[116] Studies conducted by X. Li *et al.*, demonstrated the fabrication of GelMA with tuneable mechanical properties that can be achieved based on different DS of GelMA. The mechanical stiffness of GelMA ranged from 3.8 ± 0.3, 17.1 ± 2.4, and 29.9 ± 3.4 kPa for low, medium and high DS of GelMA, respectively. Similarly, the microporous properties of GelMA are essential to maintaining the chondrocyte phenotype and its proliferation rate.[117,118] Although the mechanical strength of GelMA hydrogel is tuneable, it is still lower compared to native cartilage tissue. Hence, a combination of hydrogel with GelMA is prepared to overcome the shortcoming.[72] The 3D bioprinting approach for cartilage tissue engineering provides a layer-by-layer biofabrication platform to control the distribution of matrix, cells and bioactive material at different zones of the 3D cartilage construct[119]. W. Zhu *et al.* developed a cartilage tissue constructs with a hydrogel combination of 10% w/v GelMA with various concentrations (5–20% w/v) of polyethylene glycol diacrylate (PEGDA) with the incorporation of Mesenchymal stem cells (MSCs), which differentiate into chondrocytes. The presence of PEGDA increases the printability of the bioink with a printing resolution of 1000 μm without PEGDA and 400 μm with 5% w/v PEGDA. The mechanical strength of the hydrogel increased 8.6 folds with the addition of 5% w/v PEGDA.[120] G. Gao *et al.*, developed a bone and cartilage tissue construct by incorporating human MSCs evenly distributed in a polymerised PEG-GelMA composite scaffold, which was bioprinted using an inkjet bioprinter. The compressive modulus of PEG-GelMA with MSCs was 35 kPa which increased to 60–70 kPa after chondrogenic and osteogenic differentiation at day 21. The MSC cell viability was more than 80% with PEG-GelMA hydrogel.[121] In a study performed by M. Costantini *et al.*, they developed three different combinations of photocurable hydrogel with alginate, gelatin methacrylamide (GelMA), chondroitin sulfate amino ethyl methacrylate (CS-AEMA) and hyaluronic acid methacrylate (HAMA). All three hydrogel combinations were bioprinted with a resolution of 100 μm with bone marrow-derived MSCs (BM-MSCs) and incubated in chondrogenic media. After 21 days, the viability of chondrogenic cells in the tissue construct was 85–90%, demonstrating that the printed scaffold supports cell growth. Further, the cells in the tissue construct showed expression of chondrogenic and osteogenic markers, which was analysed using fluorescent immunocytochemistry and RT-qPCR.[122] In a study performed by Gao *et al.*, they bioprinted a cell-free bilayered porous scaffold using a combination of GelMA and GelMA – hydroxyapatite (Hap) hydrogel for the repair and reconstruction of osteochondral defects (Fig. 9a). The bioprinted scaffold contained sufficient interfilament spacing of 0.4–0.8 mm that would support the ingrowth and regeneration of articular cartilage (Fig. 9b). The cell-free scaffold was implanted in the osteochondral defects in rabbit's joints, and the *in vivo* articular cartilage regeneration was seen within 6 to 12 weeks post-implantation (Fig. 9c). GelMA and Hap, printed with sufficient interfilamentous spacing, resulted in the ingrowth and regeneration of articular cartilage.[123] Ruiz-Cantu *et al.*, used bioprinted Polycaprolactone (PCL) support layers along with bioprinted chondrocyte-laden gelatin methacyloyl (GelMA) hydrogel for nasal reconstruction (Fig. 10a). The cell viability of 10%, 15% and 20% w/v GelMA hydrogel was almost similar (80%) and was only 3% lower than that of control (monolayer culture) (Fig. 10b). On culturing this tissue construct *in vitro* neocartilage formation was observed after 3 weeks in culture.[124] The above studies demonstrate that blending GelMA hydrogel with natural, synthetic, or ceramic biomaterial can be used to develop cartilage tissue constructs. GelMA hydrogel, being biocompatible, supports cell adhesion and proliferation, and its porous nature promotes cell infiltration. However, certain limitation with GelMA bioprinting for cartilage tissue construct is surrounding vascularization for nutrient diffusion and providing appropriate mechanical strength to mimic native cartilage to withstand the load and stresses in joints for translating into clinical application.

4.2. Bone

An adult human body consists of 206 bones, which provide structure and mechanical support for soft tissues such as muscles and lungs. These are composed of connective tissue supported with calcium and specialised bone cells such as osteoblasts, osteocytes, and osteoclasts. Bones contain bone marrow, which produces blood cells. Cortical and trabecular are two types of bone found in the body. Cortical bones form the outer layer of the bone, and it is dense and compact, whereas trabecular bone forms the inner layer of the bone, and it appears spongy and honeycomb-shaped.[125] The most common causes of bone defects or injuries are ageing, infection, and failed surgical reconstruction of a joint. It is well known that bone has high regeneration potential; however, healing is not complete when the defect is larger than the critical size. Allografts or xenografts are frequently used for bone repair but are limited due to donor shortage, risk of

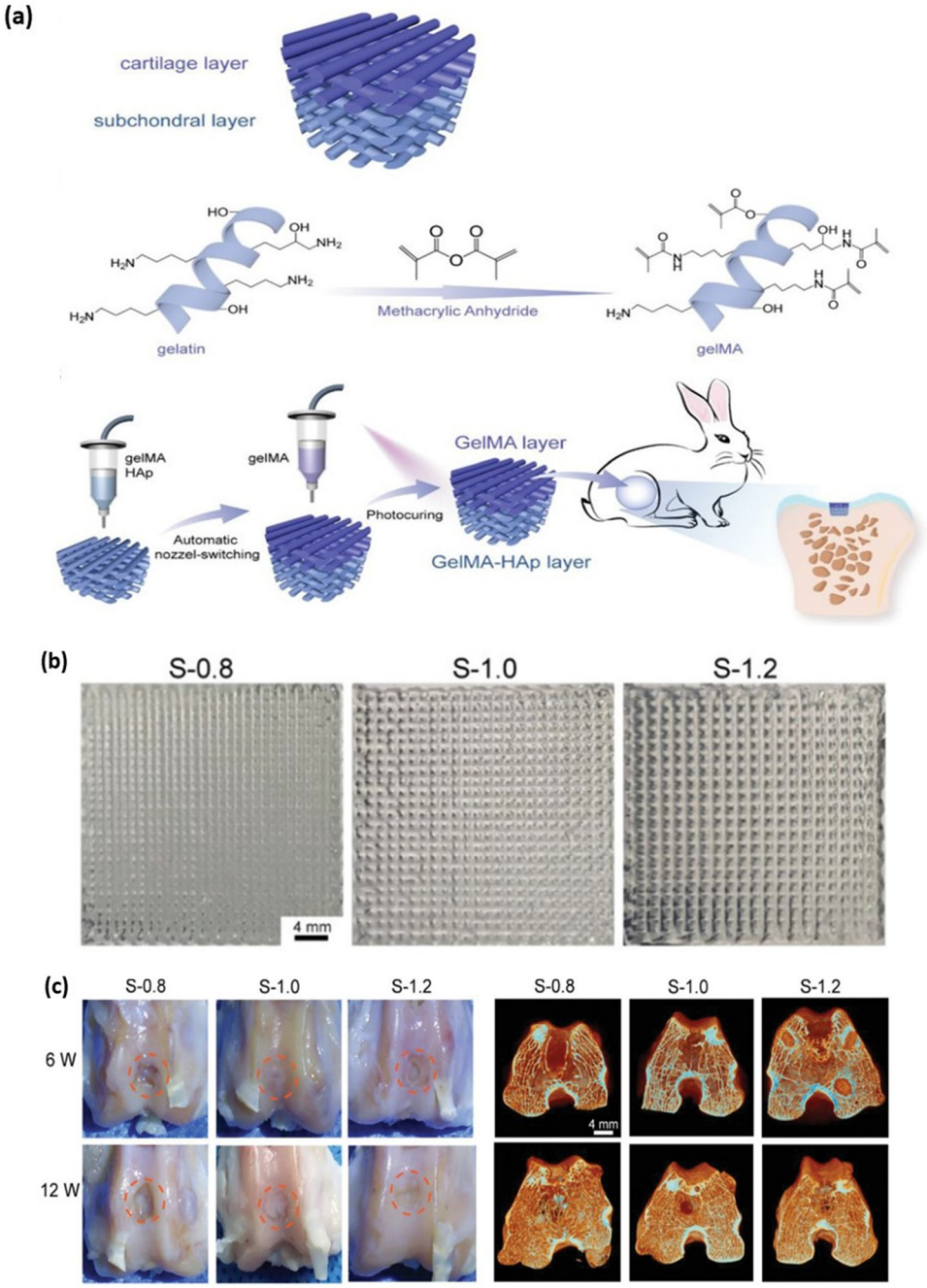

Fig. 9 Fabrication of a 3D bioprinted osteochondral bilayered cell-free scaffold using GelMA – hydroxyapatite (Hap) composite hydrogel. (a) Schematic representation for the fabrication of bilayered scaffold and its application in osteochondral regeneration in a rabbit model. (b) Image representation of the top-view of the printed construct with different interfilament spacing 0.8 mm (S-0.8), 1.0 mm (S-1.0) and 1.2 mm (S-1.2). (c) Image representing cartilage regeneration with different interfilament spaced bioprinted construct 6 to 12 weeks post-implantation in rabbit joint. Reproduced from ref. 123 with permission from John Wiley and Sons, copyright (2020).

immunogenicity, and infection.[126] A recent development in tissue engineering, specifically 3D bioprinting of bone, aims to resolve these limitations. GelMA is one of the hydrogels which showed promising results in bone regeneration. In a study by Bayambaa *et al.*, an extrusion-based bioprinter was utilised to produce bone-like tissue constructs containing perfusable vascular lumens (Fig. 11a). They synthesised GelMA hydrogel with different degrees of functionalisation and conjugation with VEGF for promoting both vasculogenesis and osteogenesis. Incorporating VEGF-GelMA and GelMA hydrogel for a bioprinted construct resulted in the creation of a perfusable lumen with an endothelial lining in the centre. Co-cultured human mesenchymal stem cells (hMSCs) in the inner fibre developed into smooth muscles that promote endothelial

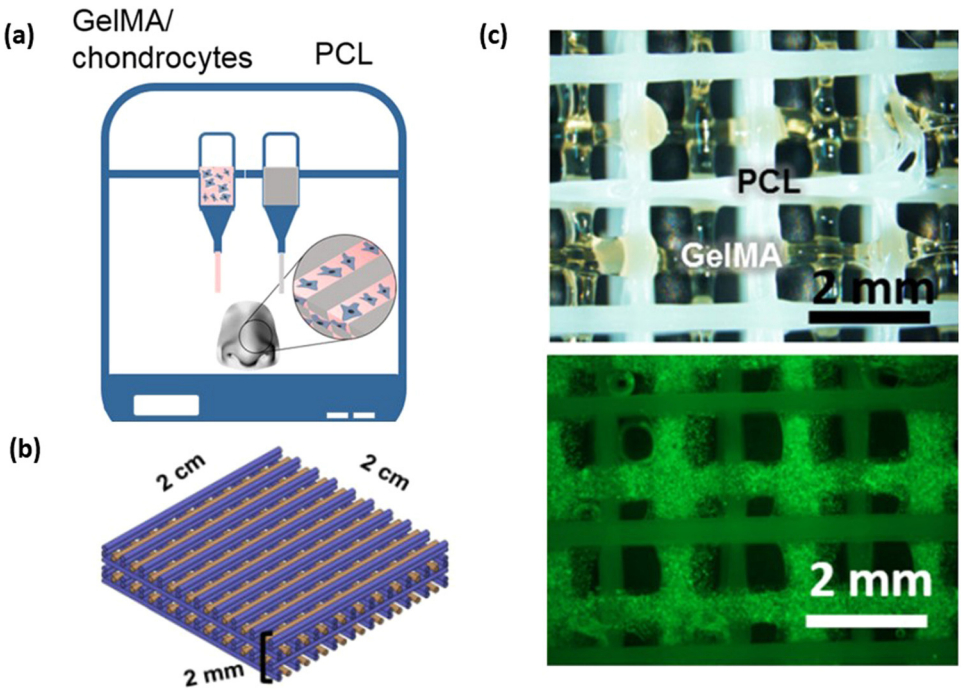

Fig. 10 3D Bioprinting of porous cartilage construct using GelMA and Polycaprolactone (PCL) composite hydrogel. (a) Schematic representation of the 3D bioprinting process using GelMA and PCL hydrogel for nasal reconstruction. (b) Schematic representation of 3D CAD design of the bioprinting construct with a combination of GelMA (orange) and PCL (blue) hydrogel. (c) Bright field image of the GelMA-PCL construct and fluorescent image showing live/dead cells. Reproduced from ref. 124 with permission from Elsevier, copyright (2020).

cell proliferation (Fig. 11b and c). Encapsulation of hMSCs and bioactive silicate nanoplatelets in GelMA-VEGF induce osteogenic differentiation *in vitro*.[127] Buyuksungur *et al.* fabricated a 3D bioprinted bone construct using polycaprolactone (PCL) and dental pulp stem cell (DPSCs) laden GelMA hydrogel (Fig. 12a). GelMA hydrogel showed osteoinductivity, while the PCL provided mechanical strength for bone formation. 90% cell viability was observed within the fabricated scaffold after 21 days of incubation (Fig. 12c), and the Alizarin red staining method confirmed the osteogenic differentiation of DPSCs. The osteogenic differentiated DPSCs also expressed collagen type I, osteopontin and osteocalcin protein markers within the fabricated construct which was analysed from day 7 to day 21.[128] In another study by Allen *et al.*, an extrusion-based 3D bioprinter was used to fabricate a porous scaffold containing MC3T3-E1 subclone 4 mouse calvarial osteoblast cells and GelMA-gelatin with hydroxyapatite (Hap) for bone tissue engineering.[129] After 28 days of culturing, various analysis was conducted. The results indicated that GelMA-gelatin hydrogel reinforced with Hap extensively reduced hydrogel swelling by 80–100 times compared with only GelMA hydrogel. The hydrogel's ability to resist collagenase IV degradation was significantly improved compared to GelMA hydrogel where after 28 days the mass loss was greater than 90% for GelMA and only 23–17% for GelMA-Hap. The osteoblastic differentiation and mineralisation were enhanced with the osteogenic gene expression level of Bone Morphogenetic Protein 7 (BMP7), and osteocalcin was upregulated. In comparison with GelMA-gelatin hydrogels, GelMA-Hap hydrogel had two times the cell proliferation and similar cell viability (80%).[130] In another study by Cidonio *et al.*, LAPONITE® nanoclay (LPN) and GelMA were combined to produce a hydrogel that exhibits excellent shape retention post-swelling. Adding 0.5% w/v LPN to 7.5% w/v GelMA increased the mass swelling ratio from 20 to 60. Higher drug retention and slower release were observed with LPN-GelMA compared to GelMA-only hydrogel. Bioprinted 3D cell-laden constructs showing a cell viability of 76.12 ± 10.93%. Adding LAPONITE® leads to higher cell proliferation from day 7 to day 21. Further, the osteogenic differentiation was higher in LPN-GelMA hydrogel compared to GelMA hydrogels, which were analysed with Alizarin Red staining and extensive mineral deposition.[131] For bone regeneration, GelMA hydrogels are blended with bioactive ceramic biomaterials to induce mineralization or blended with other polymers to improve their mechanical properties for bone tissue engineering applications. However, maintaining the long-term viability and stability of bioprinted bone within the body, especially for load-bearing applications, is still challenging.

4.3. Cardiac tissue

The heart is the organ in the body that pumps blood throughout the body. Cardiac muscles consist of three main cell components: cardiomyocyte, cardiac fibroblast, and endothelial cells. Cardiac fibroblasts maintain the structural integrity of cardiomyocytes and produce a large number of cardiac extracellular proteins.[129] The heart has three types of cardiac tissue:

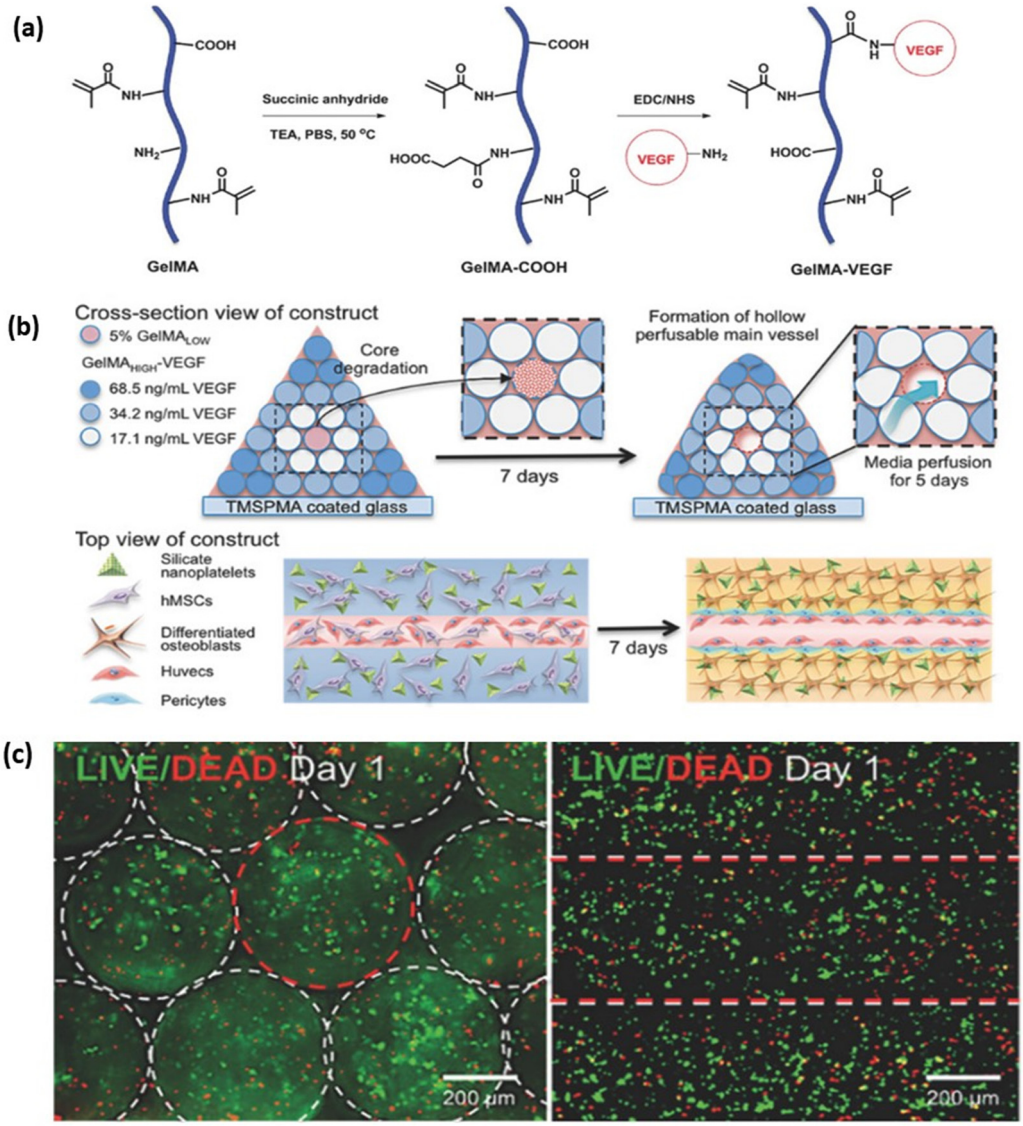

Fig. 11 3D bioprinting of vascularised bone tissue construct within a GelMA-based biomatrix along with Human Umbilical Vein Endothelial Cells (HUVACs) and Bone Marrow derived Mesenchymal Stem Cells (BM-MSCs). (a) Schematic representation of the modification of GelMA hydrogel for bioink preparation. (b) Schematic representation of the 3D printing process and the arrangement of cells within the 3D bioprinted construct. (c) The cell viability at day one within the 3D hydrogel construct using live/dead staining. Reproduced from ref. 127 with permission from John Wiley and Sons, copyright (2017).

myocardium, endocardium, and pericardium. The outermost layer of the heart wall is made of a thick muscular layer called myocardium, composed of cardiomyocytes. Sinoatrial Node (SAN), known as the heart's pacemaker, can induce myocyte contraction without nerve stimulation.[132] Anisotropic alignment of the myocytes leads to the electrical activation of the cardiac muscles. The innermost layer of the heart is the endocardium, composed of endothelial cells and forms overlapping regions that help seal the heart and connect the blood vessels around it. The pericardium is a fibroserous sac surrounding the heart and the blood vessels. It contains pericardial fluid that acts as a lubricant for the membranes to slide over one another in the pericardial activity.[133] Cardiac tissue engineering has been a growing interest because of heart failure, myocardial infarction (MI) and congenital heart defects. These heart conditions are more likely to experience cardiac dysfunction, leading to more significant morbidity and mortality.[134] In recent years, 3D bioprinting has proven to be a promising option for regenerating functional cardiac tissues. In a study by Duan *et al.*, the researchers developed a 3D bioprinted heart valve conduit based on methacrylated hyaluronic acid (Me-HA)/GelMA hydrogels (Fig. 13a). This hybrid hydrogel helps regulate encapsulated human aortic vascular interstitial cell (HAVICs) behaviours (Fig. 13b). These bioprinted valve conduits maintained their structure for seven days in static culture (Fig. 13c) and had greater than 90% cell viability of cells encapsulated at a depth of 700 μm (Fig. 13d). The expression of αSMA and vimentin in the heart conduit

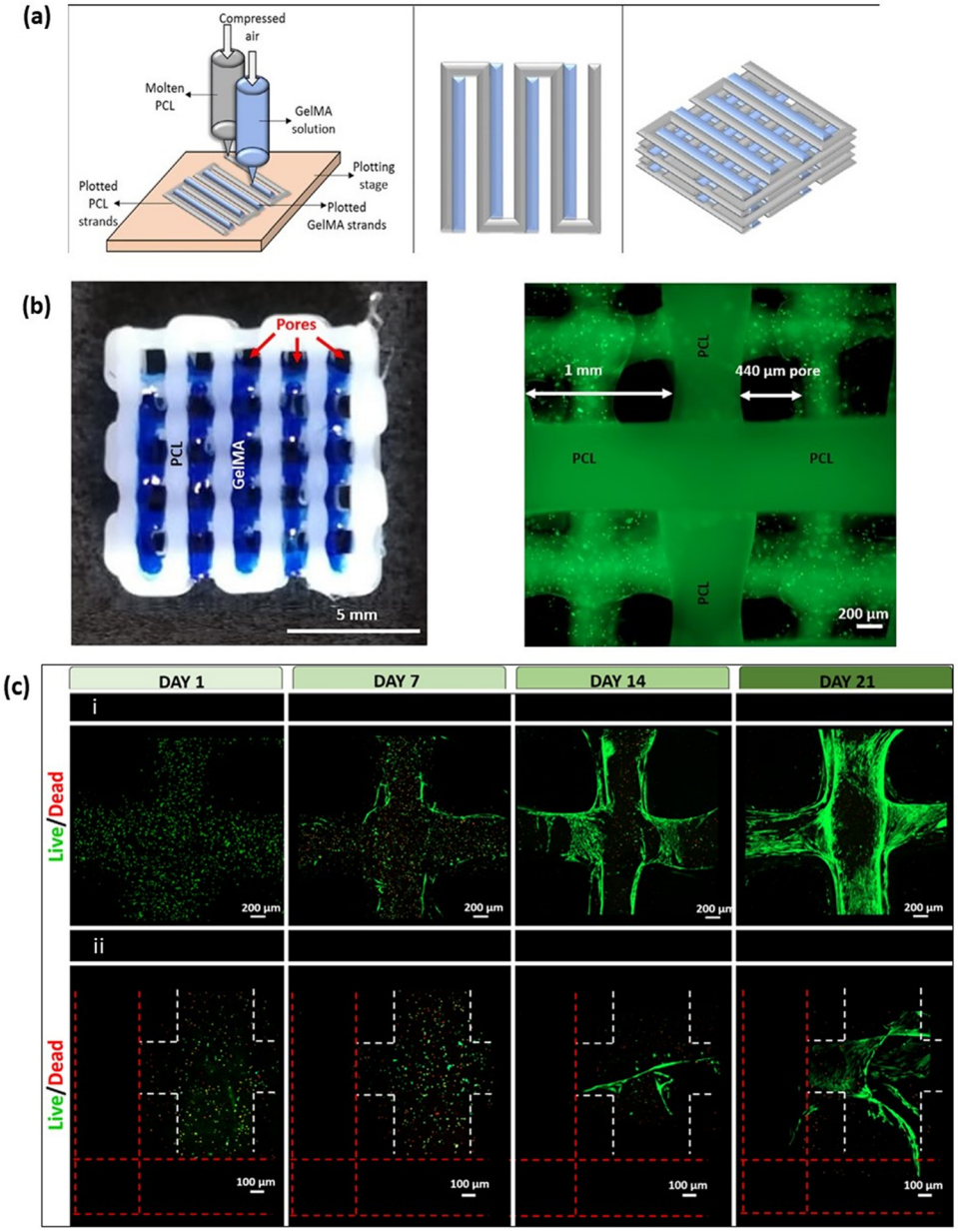

Fig. 12 Fabrication of 3D bioprinted bone construct with a combination of polycaprolactone (PCL) and dental pulp stem cells (DPSCs) laden GelMA hydrogel. (a) Schematic representation for the fabrication of a 3D bioprinted hybrid hydrogel bone construct. (b) Stereomicrograph image of the bioprinted construct with DPSCs laden GelMA stained with Brilliant Blue (left) and a fluorescent image depicting the presence of DPSCs within GelMA hydrogel stained with Alexa Fluor™ 488 phalloidin. (c) Live/dead analysis of DPSCs laden GelMA hydrogel at different periods (1, 7, 14 & 21 days). (i) DPSCs laden GelMA scaffold. (ii) DPSCs laden GelMA – PCL hybrid scaffold (PCL border depicted in red dotted lines). Reproduced from ref. 128 with permission from John Wiley and Sons, copyright (2021).

confirmed the activation of HAVICs.[135] In another study by Bejleri *et al.*, the researchers developed a bioink by combining cardiac progenitor cells (CPCs) extracted from patients and decellularised cardiac extracellular matrix hydrogel (dECM) with GelMA (Fig. 14a). The bioprinting of GelMA-dECM showed better printability (1.0) compared to only GelMA hydrogel (0.95). Here, a printability value close to 1.0 suggests that the bioink has an ideal printing property with homogenous filament thickness, interfilament gap and rigid multiple stack construct (Fig. 13b). The mechanical stiffness of GelMA-dECM was 5000 Pa, which was similar to the stiffness of native myocardium. After bioprinting and *in vitro* culture, the dECM scaffolds showed significantly higher gene expression of cardiac markers than GelMA-bioprinted scaffolds. In the *in vivo* study, GelMA with dECM was implanted in the hearts of the rats, and the patch maintained its shape with blood vessel infiltration into the patches after 14 days.[136] Zhu *et al.* developed a new bioink to encapsulate cardiomyocytes using alginate, GelMA and gold nanorods (GNR). Centrimethylammonium bromide (CTAB) was used to coat nanorods to

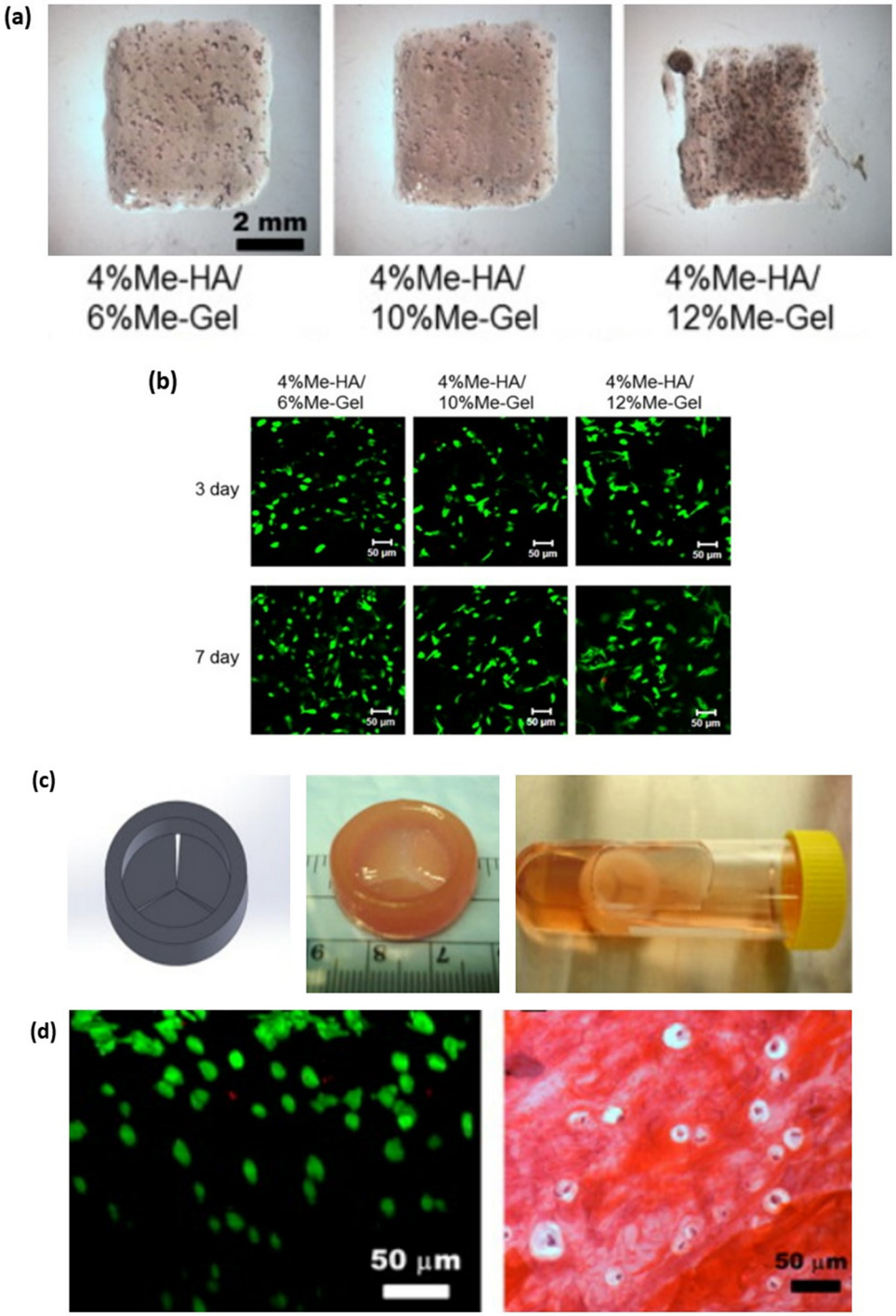

Fig. 13 3D bioprinting of trileaflet valve conduit using methacylated hyaluronic acid (Me-HA) and methacrylated gelatin (GelMA) hydrogel and human aortic valvular interstitial cells (HAVICs). (a) Image representing bioprinted construct with different combination of Me-HA and GelMA hydrogel. (b) Biocompatibility studies of different hydrogels encapsulated with HAVICs using live/dead cell staining assay. (c) Computer-aided design of heart valve conduit and 3D bioprinted HAVICs encapsulated heart valve conduit kept in 7 days static culture. (d) Live/dead cell images of HAVICs within the valve conduit and histological staining of bioprinted valve conduit after seven days in culture. Reproduced from ref. 135 with permission from Elsevier, copyright (2014).

prevent them from aggregating, and GelMA helps improve the hydrogel's biocompatibility. After day 1, 0.1–0.25 mg ml^{-1} GNR concentration with 7% w/v GelMA showed the maximum cell retention (more than 50%) than GelMA hydrogel (20%). The cellular studies showed a cell viability of 70% and were maintained across all layers of the printed structure. GNRs significantly influenced cardiomyocyte proliferation and spread after 12 days of culture. The researchers successfully printed constructs and implanted cardiac tissue using GelMA scaffolds. They observed that only a tiny quantity of GNRs could enter the

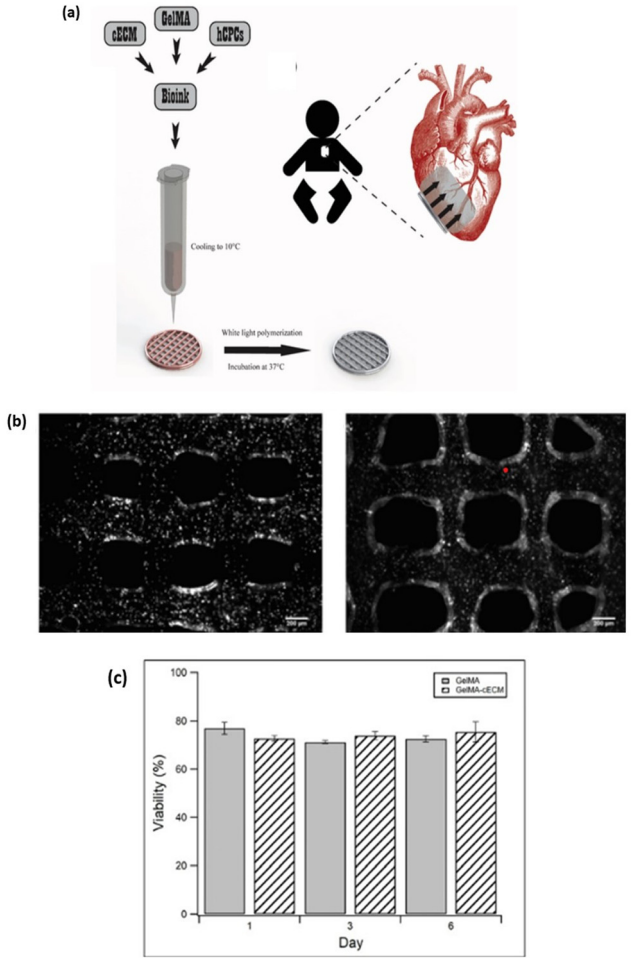

Fig. 14 3D Bioprinting of cardiac patch with a formulated bioink composed of cardiac extracellular matrix (cECM), GelMA and human cardiac progenitor cells (hCPCs). (a) Schematic representation of bioink formulation and bioprinting process for fabricating the cardiac patches. (b) Bright field image showing the cell-laden bioprinted construct using only GelMA hydrogel (left) and a combination of GelMA-cECM hydrogel (right). (c) Biocompatibility studies using live/dead fluorescent assay of cell-laden GelMA construct (left), cell-laden GelMA-cECM construct (right) and a graph representing the cell viability within the two bioprinted constructs. Reproduced from ref. 136 with permission from John Wiley and Sons, copyright (2018).

bloodstream after the degradation of GelMA scaffolds.[137] GelMA hydrogel has shown promise in fabricating cardiac tissue constructs such as valves and cardiac patches. GelMA provides a biocompatible matrix for cardiac cells to grow and proliferate, and in combination with bioactive molecules, nanoparticles and growth factors, specific cardiac functions can be achieved. The main challenge is to promote vascularization within the cardiac tissue and a material system that can withstand dynamic contraction and relaxation for clinical application.

4.4. Skeletal muscle

Skeletal muscle is one of the most flexible tissues in the human body and accounts for 40% of total body weight. The skeletal muscles are connected to the bone with the help of tendons, which are essential for body movements. The skeletal muscles are made up of thousands of muscle fibres that are bound together by connective tissue sheaths. Muscle fibres are made up of myofibrils containing multiple myofilaments. Sarcomeres, the basic contractile unit of skeletal muscles, are formed when the myofibrils are all bundled together in a single-striated pattern.[138] Actin and myosin are the two significant myofilaments arranged in a way that forms various bands on the skeletal muscles.[139] Functions of skeletal muscle include providing structural support, maintaining a proper body posture, and attachment to the bones *via* tendons, which helps in body movement. Skeletal muscles have a self-healing capacity where minor injuries can be resolved by themselves, but in the case of significant trauma or extensive injuries, the injuries are not resolved by themselves.[140] The 3D bioprinting approach can be utilised to repair extensive injuries. Various studies have combined GelMA hydrogel and other biomaterials to develop 3D bioprinted skeletal muscles. In a study by Kim and Kim, they developed a GelMA-based functional hydrogel to fabricate a biocompatible and functional cell-laden structure that mimics native muscle tissue. The cell-laden GelMA hydrogel was loaded in a syringe and incubated in a CO_2 incubator at 37 °C, 5% CO_2 for 0 (GelMA-0), 3 (GelMA-3), 5 (GelMA-5) and 7 (GelMA-7) days. An extrusion nozzle was used to print the cell-laden bioink to evaluate the cell viability and morphology (Fig. 15a). The cell viability of GelMA-0, GelMA-3, and GelMA-5 corresponding to cell-laden GelMA incubated at day 0, day 3 and day 5 was more than 90% but the viability decreased to lower than 30% after day 7 (GelMA-7) due to a decrease in cell nutrition. The myoblast cell morphology with GelMA-0 (day 0) showed random orientation of myotube, whereas GelMA-5 (day 5) had uniaxial orientation after bioprinting, leading to a significantly higher degree of myotube orientation/formation and myogenic gene expression for printed constructs compared to non-printed cell-laden constructs (Fig. 15b).[141] In another study by García-Lizarribar *et al.*, the researchers developed three different combinations of GelMA bioink for the regeneration of skeletal muscles, which include GelMA-alginate-methacrylate (GelMA-AlgMA), GelMA-carboxymethyl cellulose-methacrylate (GelMA-CMCMA), and poly(ethylene glycol) diacrylate-added GelMA (GelMA-PEGDA) bioinks (Fig. 16a). GelMA has advantages such as high biocompatibility and crosslinking properties but has certain limitations, such as poor mechanical properties and degradation resistance. Incorporating several polymers such as alginate, CMC, and PEGDA, overcame these limitations. In contrast, GelMA-PEGDA, GelMA-CMCMA and GelMA-AlgMA were more resistant to degradation and maintained their 3D structure with more than 68% of the mass remaining after 4 hours compared to GelMA. Using GelMA, GelMA-AlgMA and GelMA-CMCMA as bioink for skeletal muscle tissue engineering did not interfere with the growth of C2C12 myoblasts, proliferation, and alignment. GelMA-AlgMA and GelMA-CMCMA maintained relative cell viability of 80%, whereas with GelMA-PEGDA the viability decreased to 40% owing to a reduction in pore size, thus affecting nutrient diffusion (Fig. 16b and c)[142]. In another experiment by Seyedmahmoud

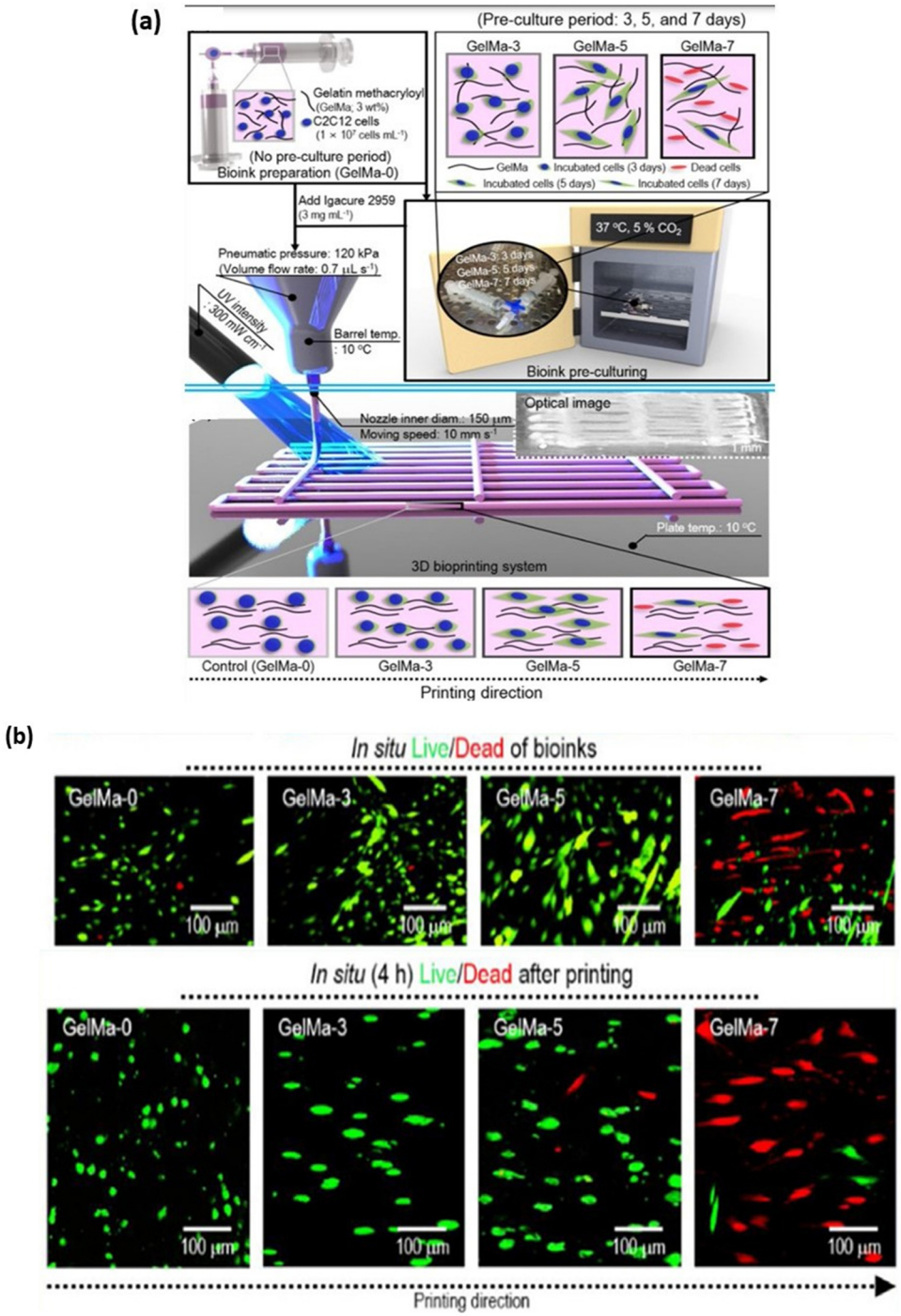

Fig. 15 3D bioprinting of cell-laden GelMA bioink to achieve C2C12 myoblast cell alignment and maturation within the 3D construct. (a) Schematic representation of bioink preparation, the cellular viability and morphology within the bioink with or without pre-incubation and cellular alignment after the bioprinting process. (b) Live/dead cell viability analysis within the pre-incubated bioink and 4 hours after the bioprinting process. Reproduced from ref. 141 with permission from Elsevier, copyright (2020).

et al., the researchers developed a 3D muscle construct using GelMA-alginate bioink through UV exposure and ionic crosslinking for skeletal muscle tissue engineering[143]. The result demonstrated that GelMA-alginate bioink crosslinked with UV and $CaCl_2$ provided a suitable environment for muscle tissue formation with comparable cell viability to GelMA-only bioink. It was observed that electrical stimulation of a minimum of 1 V cm^{-1} for one day in culture increased muscle myotube maturation and improved alignment. Adding an oxygen-generating source to GelMA bioink helps improve the cells' metabolic activity. Bioprinted muscle constructs may be widely used in drug screening and tissue regeneration.[144] The above studies

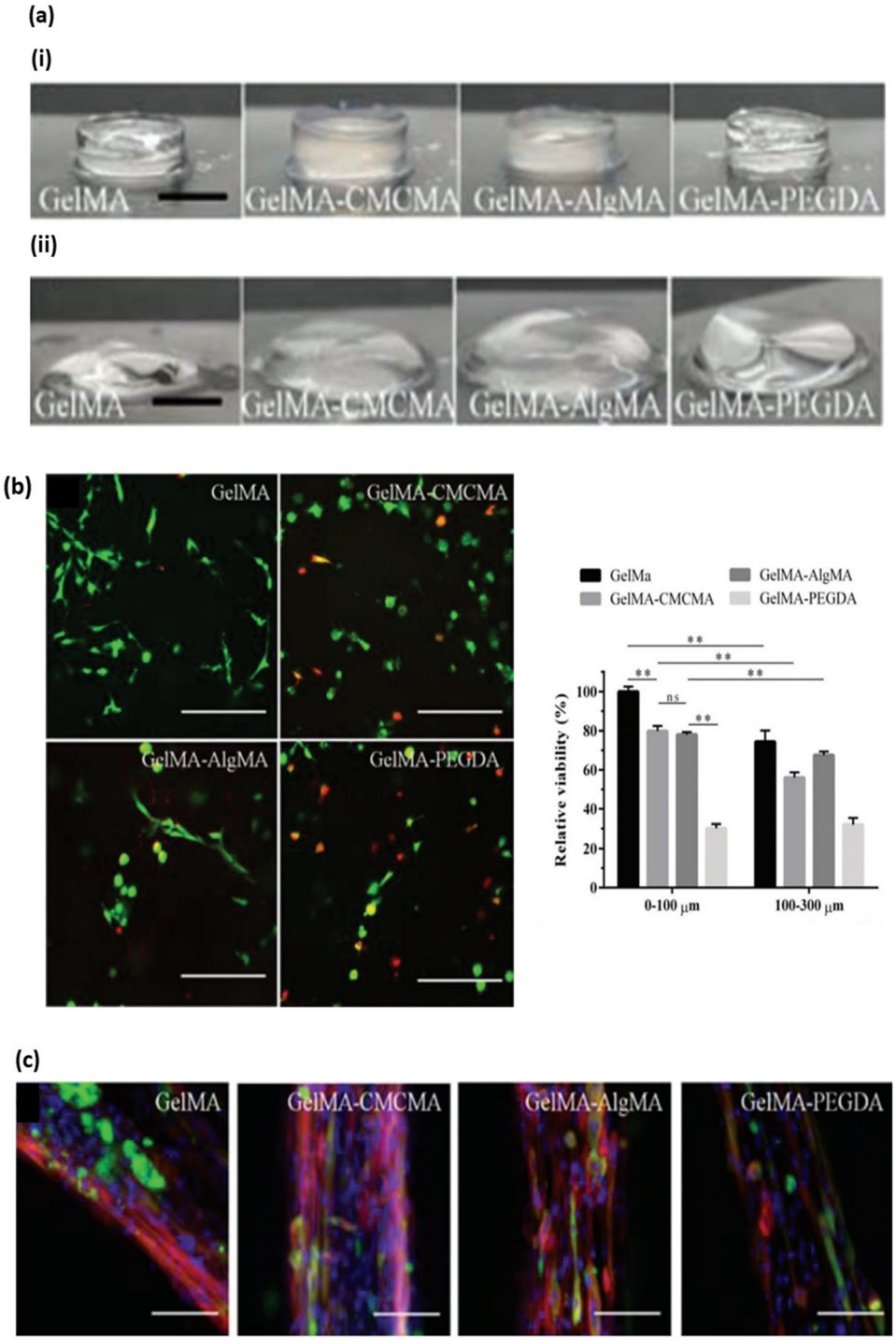

Fig. 16 3D Bioprinting of a composite biomaterial composed of GelMA bioink in combination with alginate methacrylate (AlgMA), Carboxymethyl Cellulose Methacrylate (CMCMA) and poly(ethylene glycol) diacrylate (PEGDA) for the fabrication of a highly aligned muscle tissue construct with C2C12 myoblast cells. (a) Fabrication of 5% w/v GelMA composite hydrogel constructs crosslinked *via* different photoinitiators. (i) Lithium phenyl (2,4,6-trimethylbenzoyl) phosphinate (LAP). (ii) 2-Hydroxy-4′-(2-hydroxyethoxy)-2 methylpropiophenone (I2959. (b) Biocompatibility analysis of different composite hydrogels using live/dead fluorescence viability assay. (c) Confocal Image representing myotube formation with encapsulated C2C12 cells in the bioprinted construct stained for F-actin (red), Myosin heavy chain (green) and nuclei (blue). Reproduced from ref. 142 with permission from John Wiley and Sons, copyright (2018).

demonstrate the use of GelMA hydrogels for skeletal tissue engineering and support the formation of myofilaments and myotubes. The 3D bioprinting technique further allows the formation of tissue constructs with a uniaxial and aligned orientation of myofilament, which is advantageous for developing muscle tissue constructs. The major limitation for

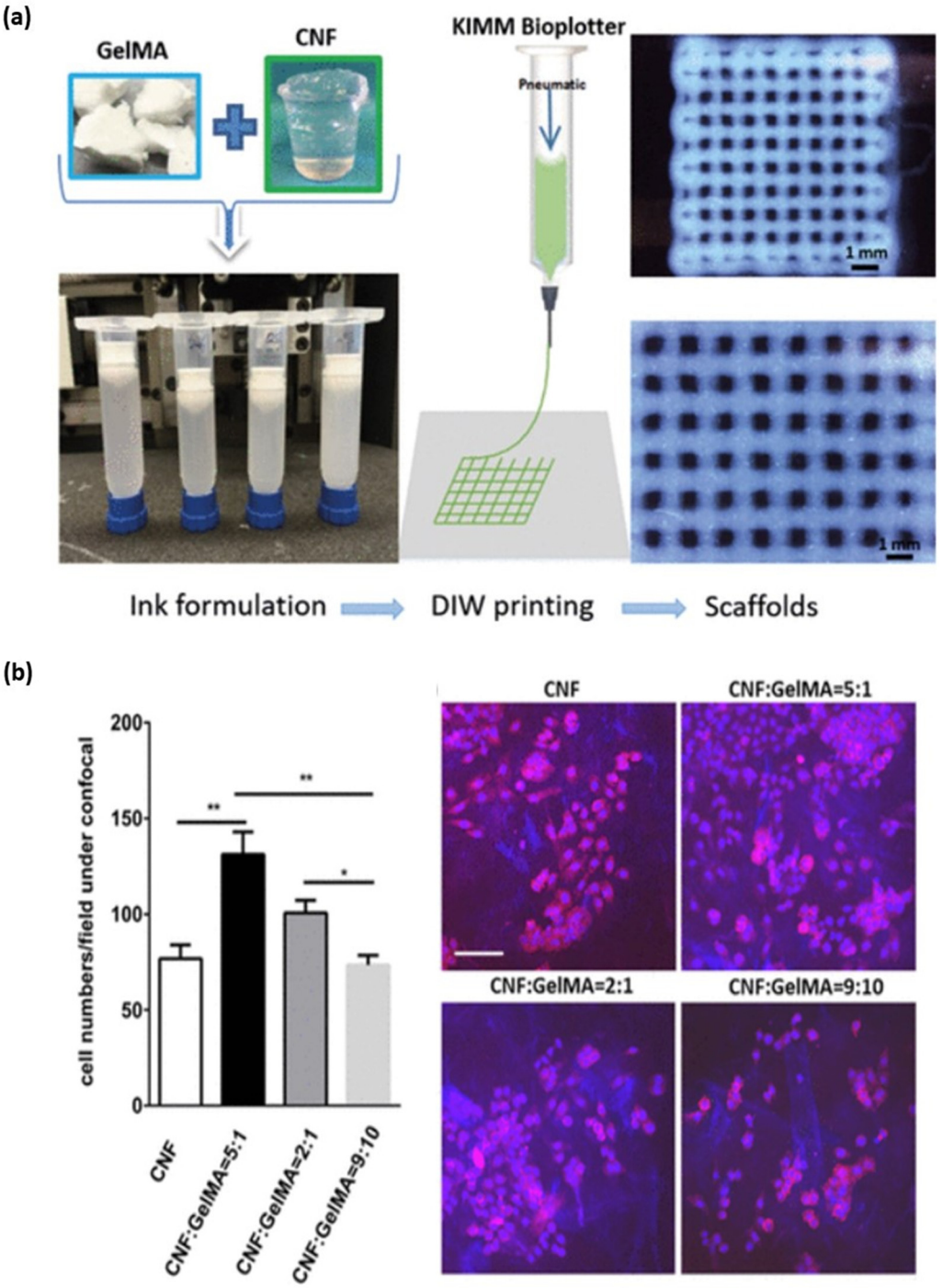

Fig. 17 3D bioprinting of skin tissue construct for wound healing application using composite bioink formulation of cellulose nanofibrils (CNF) and GelMA hydrogel with 3T3 fibroblast cell lines. (a) Image representing the formulation of CNF – GelMA bioink and the bioprinting process to fabricate the designed scaffold. (b) Confocal cell viability and proliferation study of cell-laden CNF and CNF-GelMA composite hydrogel construct stained with Phalloidin-DAPI fluorochrome observed after three days. Reproduced from ref. 149 with permission from American Chemical Society, copyright (2019).

fabricating muscle tissue constructs is achieving muscle contractility, which is essential for clinical application.

4.5. Skin

Skin is the largest and most exposed organ of the human body. It acts as a protective barrier against various infections and helps regulate body temperature. It consists of three layers: the epidermis, dermis, and hypodermis.[145] The epidermis is the skin's outermost layer containing melanocytes and keratinocytes. The melanocytes in the epidermis produce melanin pigment that gives the colour composition of the skin. The keratinocytes form a barrier to prevent foreign substances from

entering the body. They are highly specialised and produce keratin, cytokines, and growth factors.[146] The dermis is the second layer of the skin, consisting predominantly of collagen and fibroblast. Collagen provides an extracellular matrix to properly support fibroblast cells and structural integrity for the dermal layer; elastin makes the skin flexible. The hypodermis is the bottom layer of the skin containing adipose tissue, mainly the fat tissues and blood vessels.[143] Acute and chronic factors, including burns, ulcers, and traumatic postsurgical wounds, can cause skin injuries. Skin repair is usually done through skin grafts or reconstructive surgery, but these have certain limitations, like the availability of donor skin and, in the case of flap surgery, the creation of new wound sites in patients.[147] 3D bioprinting technology can be used for treatment by making a new skin construct mimicking the native tissue properties. GelMA is used widely for skin bioprinting

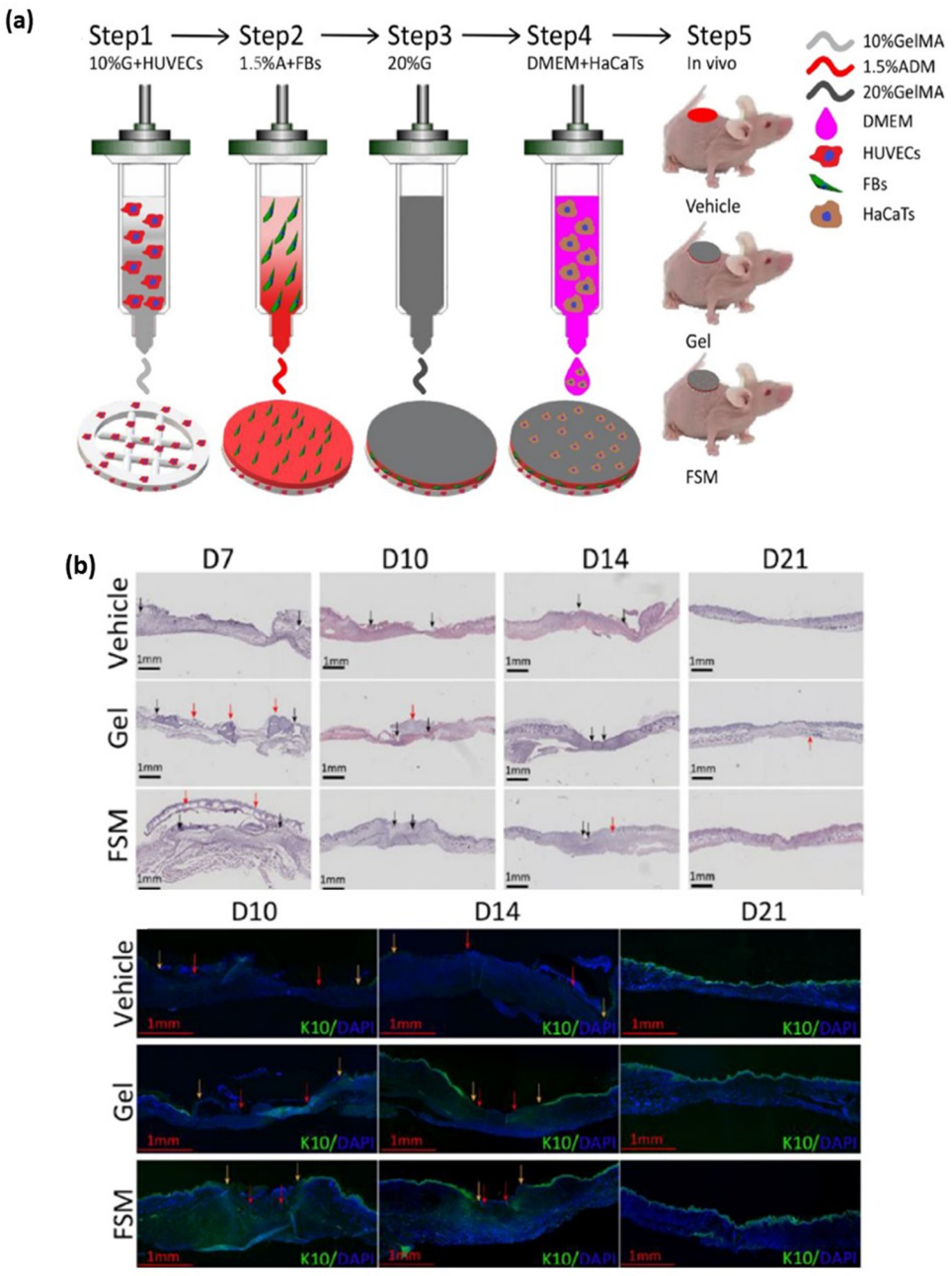

Fig. 18 3D Bioprinting of full-thickness skin construct using the hydrogel components as an acellular dermal matrix (ADM) and GelMA with cellular components of fibroblast and HUVACs as dermal and immortalised keratinocytes cell line (HaCaTs) for epidermal construct fabrication. (a) Schematic representation of the 3D bioprinting process for fabricating layer-by-layer functional skin model (FSM) with different bioink formulation and their application in wound healing. (b) H&E staining of wound tissue area and Keratin 10 (K10) immunofluorescent analysis of epidermal integrity during the wound healing process. Reproduced from ref. 150 with permission from Elsevier, copyright (2021).

because of its excellent biocompatibility and crosslinking properties. In a study performed by Shi *et al.*, the researchers developed a collagen-doped tyrosinase (Ty) incorporated into GelMA-based bioink. They used three different skin cells, human melanocytes (HEM), human keratinocytes (HaCat), and human dermal fibroblasts (HDF), to study the biological behaviour of the printed construct. They used two-step crosslinking methods to enhance the mechanical strength and printability of bioink. In the first step, collagen was crosslinked enzymatically using tyrosinase, followed by photo-crosslinking of GelMA. With the addition of 800 U ml^{-1} tyrosinase, the storage modulus increased from 500 Pa (at 0 U ml^{-1} tyrosine) to 2000 Pa. Cell viability of above 90% was seen across all bioink compositions with all skin cell types till day 14. The *in vivo* test result indicated that the wound healing rate improved with tyrosinase-doped bioink with total wound closure at day 14.[148] Xu *et al.*, used a dual crosslinking strategy for improving the mechanical properties of GelMA hydrogels for wound healing. They developed a hydrogel using low-concentration GelMA and 2,2,6,6-tetramethylpiperidine-1-oxyl (TEMPO)-oxidised cellulose nanofibrils (CNF). Dual crosslinked hydrogel was prepared by UV crosslinking of GelMA followed by ionic crosslinking of CNF with Ca^{2+} (Fig. 17a). The results demonstrated there was an improved mechanical strength of the hydrogel with an increased concentration of GelMA. The Young's modulus of 5 : 1 CNF : GelMA was 2.3 kPa, which increased to 4.5 kPa at 9 : 10 CNF : GelMA hydrogel construct. The cell viability of 3T3 fibroblast cells was more than 90% in the printed construct (Fig. 17b). This bio-ink was an appropriate candidate for wound healing applications.[149] Jin *et al.*, developed a full-thickness functional skin model (FSM) using an acellular dermal matrix and GelMA. The bioprinting process of full-thickness skin model by layer-by-layer deposition of GelMA bioink encapsulated with HUVEC and dermal fibroblast, which is then used for wound healing (Fig. 18a). The bioink showed excellent biocompatibility and tunable mechanical properties. *In vitro* results confirmed that the 3D-printed full-thickness FSM can provide an optimum microenvironment for cell growth and promote cell viability and proliferation. *In vivo* analysis demonstrated the effect of FSM after implanting it into the excision wounds. The result showed the survival of printed cells, re-epithelization, dermal ECM secretion and angiogenesis, thus promoting wound healing (Fig. 18b)[150]. GelMA hydrogels are excellent candidates for skin tissue engineering and support many skin cell types like human melanocytes, human keratinocytes and human dermal fibroblast and promote wound healing in in-vivo animal models. Further, by varying the crosslink concentration, the mechanical properties of GelMA can be varied to match that of native skin tissue. GelMA hydrogels can also be incorporated with bioactive molecules such as decellularized ECM and growth factors to enhance their biological properties. Although 3D bioprinting of GelMA hydrogels has shown promise, challenges like vascularization of the tissue construct and host immune response must be addressed before clinical applications.

GelMA hydrogel has provided an ideal material for fabricating various tissue constructs. The advantages of GelMA for fabricating different tissue constructs are summarized in

Table 5 Advantage of GelMA in 3D bioprinting of various tissue construct

Tissue construct	Biopolymer composite	Advantage of GelMA	Ref.
Cartilage	GelMA – bacterial nanocellulose (BNC)	• Can be physiochemically tuned by photo-crosslinking. • Better 3D printing fidelity of different shapes for cartilage repair.	151
	GelMA – PLA	• Improve cell viability and promote *in vivo* articular cartilage regeneration	152
	GelMA/silk fibroin-gelatin (SF-G)	• 2.5 folds more PRG4 expression level corresponding to articular cartilage markers seen with GelMA bioprinted construct	153
Bone	GelMA – HAp	• Promote cell attachment and increase cell viability. • Induce osteogenic differentiation of MC3T3-E1 cells	154
	GelMA – gellan gum methacrylate (GGMA)	• Printing fidelity and mechanical support for 3D bioprinted bone construct. • Photo-crosslinked hydrogel network providing sustained drug release for vascularization and osteogenic differentiation.	155
	GelMA-reduced graphene oxide (rGO)	• Provide cell adhesion and cell viability. • High expression of osteogenic and neural protein markers.	156
Cardiac	GelMA-methacrylated hyaluronic acid (MeHA)-decellularized human heart ECM (dhECM)	• Improve the printability of the composite hydrogel.	157
	GelMA – collagen methacrylate (ColMA) – fibronectin (FN) – laminin (LN)	• Improve the printability of the hydrogel. • Increases cell viability.	158
	GelMA – methacrylated hyaluronic acid (HAMA)	• Helps maintain valve interstitial cells (VIC) in the quiescent stage and induces differentiation into disease phenotype under cytokine and calcifying stimulus.	159
Skeletal muscle	GelMA – collagen – dECM	• Stimulate myogenic differentiation and upregulation of myogenic genes (MHC and troponin T) when cell-laden GelMA was printed in topological cue to induce cell alignment.	160
	GelMA – fibrinogen	• Photocuring helps develop interpenetrating networks with tunable viscoelasticity with faster stress relaxation properties and cell viability.	161
	GelMA – AlgMA – fibrin	• Improve printability of hydrogel and tunable mechanical properties. •Induce myogenic differentiation	162
Skin	GelMA – silk fibroin	• Closely mimic native ECM matrix to promote cell attachment and proliferation.	163
	GelMA – nanocellulose	• Improves thermal stability and biocompatibility characteristics of bioink.	164
	GelMA – HAMA – adipose-derived dECM	• Aids in cell attachment and proliferation within the scaffolds.	165

Table 5. GelMA hydrogels are a versatile biomaterial for fabricating tissue constructs using a 3D bioprinting approach.

Conclusion

Biofabrication is an emerging area of research and has made significant advancements to develop functional tissue in tissue engineering. It involves depositing cells, biomaterials, and bioactive molecules to fabricate a 3D tissue model mimicking the native tissue. The architecture of the fabricated structures still has limitations compared to native tissue. However, these structures have shown promising results in the regeneration of various tissues. More researchers are interested in exploring this technology and the use of various biomaterials for 3D bioprinting. Gelatin methacryloyl (GelMA) shows promising results in tissue regeneration. GelMA hydrogel has been found to be a potentially useful biomaterial for various biomedical applications due to its simplicity, cost-effectiveness, biocompatibility, crosslinking ability, and tuneable physiochemical properties. The studies discussed in the review conclude that GelMA is an excellent bioink candidate for developing bioprinted functionalised living tissues. In the coming years, bioprinting will likely be one of the most exciting and promising areas in tissue engineering, with newer studies discussing the clinical translation of printed GelMA constructs for tissue regeneration.

Author contributions

Conceptualization: R. N. Ghosh, M. Peter and J. Thomas; formal analysis: R. N. Ghosh; funding acquisition: M. Peter, P. K. Namboothiri and J. Thomas; methodology: R. N. Ghosh and J. Thomas; supervision: M. Peter; writing – original draft: R. N. Ghosh, Devi N. G, A. Janardanan and Vaidehi B. R; writing – review and editing: R. N. Ghosh, M. Peter, P. K. Namboothiri and J. Thomas; All authors have read and agreed to the published version of the manuscript.

Conflicts of interest

The authors wish to declare that Joseph Thomas and Mathew Peter are related by family.

Acknowledgements

The authors thank the Manipal Academy of Higher Education, Centre for Doctoral Studies-Intramural Fund-2019 and seed grant for their financial support.

References

1 R. Lanza, R. Langer, J. Vacanti and A. Atala, *Principles of Tissue engineering*, 5th edn, 2020.
2 N. de Isla, C. Huseltein, N. Jessel, A. Pinzano, V. Decot, J. Magdalou, *et al.*, Introduction to tissue engineering and application for cartilage engineering, *Bio-Medical Materials and Engineering*, IOS Press, 2010, pp. 127–133.
3 S. Caddeo, M. Boffito and S. Sartori, Tissue engineering approaches in the design of healthy and pathological in vitro tissue models, *Front. Bioeng. Biotechnol.*, 2017, **5**, 40.
4 C. Luo, H. Fang, J. Li, J. Hou, J. Yang and Q. Yuan, *et al.*, An in vivo comparative study of the gelatin microtissue-based bottom-up strategy and top-down strategy in bone tissue engineering application, *J. Biomed. Mater. Res., Part A*, 2019, **107**(3), 678–688.
5 A. Khademhosseini and R. Langer, Microengineered hydrogels for tissue engineering, *Biomaterials*, 2007, **28**, 5087–5092.
6 C. Mandrycky, Z. Wang, K. Kim and D. H. Kim, 3D bioprinting for engineering complex tissues, *Biotechnology Advances*, Elsevier Inc., 2016, vol. 34, pp. 422–434.
7 K. Hölzl, S. Lin, L. Tytgat, S. Van Vlierberghe, L. Gu and A. Ovsianikov, Bioink properties before, during and after 3D bioprinting, *Biofabrication*, Institute of Physics Publishing, 2016, vol. 8.
8 A. Panwar and L. P. Tan, Current status of bioinks for micro-extrusion-based 3D bioprinting, *Molecules*, 2016, **21**, 685.
9 T. Schmidt, Y. Xiang, X. Bao and T. Sun, A paradigm shift in tissue engineering: From a top–down to a bottom–up strategy, *Processes*, 2021, **9**, 935.
10 E. M. Ahmed, Hydrogel: Preparation, characterization, and applications: A review, *J. Adv. Res.*, 2015, **6**, 105–121.
11 W. Hu, Z. Wang, Y. Xiao, S. Zhang and J. Wang, Advances in crosslinking strategies of biomedical hydrogels, *Biomater. Sci.*, 2019, **7**, 843–855.
12 K. Y. Lee and D. J. Mooney, Hydrogels for Tissue Engineering, *Chem Rev.*, 2001, **101**(7), 1869–1880, DOI: **10.1021/cr000108x**.
13 K. Sadtler, M. T. Wolf, S. Ganguly, C. A. Moad, L. Chung and S. Majumdar, *et al.*, Divergent immune responses to synthetic and biological scaffolds, *Biomaterials*, 2019, **192**, 405–415. Available from: **https://www.sciencedirect.com/science/article/pii/S0142961218307713**.
14 A. S. Hoffman, Hydrogels for biomedical applications, *Adv. Drug Delivery Rev.*, 2012, **64**, 18–23. Available from: **https://www.sciencedirect.com/science/article/pii/S0169409X12002700**.
15 H. W. Kang, Y. Tabata and Y. Ikada, Fabrication of porous gelatin scaffolds for tissue engineering, *Biomaterials*, 1999, **20**(14), 1339–1344. Available from: **https://www.sciencedirect.com/science/article/pii/S0142961299000368**.
16 M. N. Khan, J. M. M. Islam and M. A. Khan, Fabrication and characterization of gelatin-based biocompatible porous composite scaffold for bone tissue engineering, *J Biomed Mater Res A*, 2012, **100A**(11), 3020–3028, DOI: **10.1002/jbm.a.34248**.
17 S. Sakai, K. Hirose, K. Taguchi, Y. Ogushi and K. Kawakami, An injectable, *in situ* enzymatically gellable, gelatin derivative for drug delivery and tissue engineering, *Biomaterials*, 2009, **30**(20), 3371–3377. Available from: **https://www.sciencedirect.com/science/article/pii/S0142961209003007**.

18 J. D. Kretlow, L. Klouda and A. G. Mikos, Injectable matrices and scaffolds for drug delivery in tissue engineering, *Adv. Drug Delivery Rev.*, 2007, **59**(4), 263–273. Available from: https://www.sciencedirect.com/science/article/pii/S0169409X07000282.
19 K. Yue, Trujillo-de Santiago G, Alvarez MM, Tamayol A, Annabi N, Khademhosseini A. Synthesis, properties, and biomedical applications of gelatin methacryloyl (GelMA) hydrogels, *Biomaterials*. 73, 2015. 254–271.
20 S. Xiao, T. Zhao, J. Wang, C. Wang, J. Du and L. Ying, *et al.*, Gelatin Methacrylate (GelMA)-Based Hydrogels for Cell Transplantation: an Effective Strategy for Tissue Engineering, *Stem Cell Rev. Rep.*, 2019, **15**, 664–679.
21 I. Pepelanova, K. Kruppa, T. Scheper and A. Lavrentieva, Gelatin-methacryloyl (GelMA) hydrogels with defined degree of functionalization as a versatile toolkit for 3D cell culture and extrusion bioprinting, *Bioengineering*, 2018, **5**(3), 55.
22 - AU, S. Khetan, - AU and J. Burdick, Cellular Encapsulation in 3D Hydrogels for Tissue Engineering, *J. Visualized Exp.*, 2009, **32**, e1590. Available from: https://www.jove.com/t/1590.
23 C. D. O'Connell, B. Zhang, C. Onofrillo, S. Duchi, R. Blanchard and A. Quigley, *et al.*, Tailoring the mechanical properties of gelatin methacryloyl hydrogels through manipulation of the photocrosslinking conditions, *Soft Matter*, 2018, **14**(11), 2142–2151.
24 H. Ding, N. P. Illsley and R. C. Chang, 3D Bioprinted GelMA Based Models for the Study of Trophoblast Cell Invasion, *Sci. Rep.*, 2019, **9**(1), 18854.
25 J. Yin, M. Yan, Y. Wang, J. Fu and H. Suo, 3D Bioprinting of Low-Concentration Cell-Laden Gelatin Methacrylate (GelMA) Bioinks with a Two-Step Cross-linking Strategy, *ACS Appl. Mater. Interfaces*, 2018, **10**(8), 6849–6857.
26 S. Xiao, T. Zhao, J. Wang, C. Wang, J. Du and L. Ying, *et al.*, Gelatin Methacrylate (GelMA)-Based Hydrogels for Cell Transplantation: an Effective Strategy for Tissue Engineering, *Stem Cell Rev. Rep.*, 2019, **15**, 664–679.
27 T. Jain, H. B. Baker, A. Gipsov, J. P. Fisher, A. Joy and D. S. Kaplan, *et al.*, Impact of cell density on the bioprinting of gelatin methacrylate (GelMA) bioinks, *Bioprinting*, 2021, 22.
28 Y. Wu, Y. Xiang, J. Fang, X. Li, Z. Lin and G. Dai, *et al.*, The influence of the stiffness of GelMA substrate on the outgrowth of PC12 cells, *Biosci. Rep.*, 2019, **39**(1), BSR20181748.
29 C. H. Lin, J. J. M. Su, S. Y. Lee and Y. M. Lin, Stiffness modification of photopolymerizable gelatin-methacrylate hydrogels influences endothelial differentiation of human mesenchymal stem cells, *J. Tissue Eng. Regener. Med.*, 2018, **12**(10), 2099–2111.
30 M. Costantini, S. Testa, E. Fornetti, A. Barbetta, M. Trombetta and S. M. Cannata, *et al.*, Engineering muscle networks in 3D gelatin methacryloyl hydrogels: Influence of mechanical stiffness and geometrical confinement, *Front. Bioeng. Biotechnol.*, 2017, **5**(APR), 22.
31 K. S. Lim, B. J. Klotz, G. C. J. Lindberg, F. P. W. Melchels, G. J. Hooper and J. Malda, *et al.*, Visible Light Cross-Linking of Gelatin Hydrogels Offers an Enhanced Cell Microenvironment with Improved Light Penetration Depth, *Macromol. Biosci.*, 2019, **19**(6), 1900098.
32 W. Tomal and J. Ortyl, Water-soluble photoinitiators in biomedical applications, *Polymers*, 2020, **12**, 1073.
33 N. Karaca, G. Temel, D. Karaca Balta, M. Aydin and N. Arsu, Preparation of hydrogels by photopolymerization of acrylates in the presence of Type I and one-component Type II photoinitiators, *J. Photochem. Photobiol., A*, 2010, **209**(1), 1–6.
34 Y. Lu, F. Hasegawa, T. Goto, S. Ohkuma, S. Fukuhara and Y. Kawazu, *et al.*, Highly sensitive measurement in two-photon absorption cross section and investigation of the mechanism of two-photon-induced polymerization, *J. Lumin.*, 2004, **110**(1–2), 1–10.
35 X. H. Qin, A. Ovsianikov, J. Stampfl and R. Liska, Additive manufacturing of photosensitive Hydrogels for tissue engineering applications, *BioNanoMaterials*, 2014, **15**, 49–70.
36 C. D. O'Connell, B. Zhang, C. Onofrillo, S. Duchi, R. Blanchard and A. Quigley, *et al.*, Tailoring the mechanical properties of gelatin methacryloyl hydrogels through manipulation of the photocrosslinking conditions, *Soft Matter*, 2018, **14**(11), 2142–2151.
37 P. Coimbra, D. Fernandes, P. Ferreira, M. H. Gil and H. C. de Sousa, Solubility of Irgacure® 2959 photoinitiator in supercritical carbon dioxide: Experimental determination and correlation, *J. Supercrit. Fluids*, 2008, **45**(3), 272–281.
38 T. Tozar, S. Nistorescu, M. Boni, G. Gradisteanu Pircalabioru, I. Negut and A. Staicu, Pulsed Laser Photo-Crosslinking of Gelatin Methacryloyl Hydrogels for the Controlled Delivery of Chlorpromazine to Combat Antimicrobial Resistance, *Pharmaceutics*, 2022, **14**(10), 2121.
39 N. Monteiro, G. Thrivikraman, A. Athirasala, A. Tahayeri, C. M. França and J. L. Ferracane, *et al.*, Photopolymerization of cell-laden gelatin methacryloyl hydrogels using a dental curing light for regenerative dentistry, *Dent. Mater.*, 2018, **34**(3), 389–399.
40 A. M. Rosales, S. L. Vega, F. W. DelRio, J. A. Burdick and K. S. Anseth, Hydrogels with Reversible Mechanics to Probe Dynamic Cell Microenvironments, *Angew. Chem.*, 2017, **129**(40), 12300–12304.
41 R. Holmes, X. Bin Yang, A. Dunne, L. Florea, D. Wood and G. Tronci, Thiol-ene photo-click collagen-PEG hydrogels: Impact of water-soluble photoinitiators on cell viability, gelation kinetics and rheological properties, *Polymers*, 2017, **9**(6), 226.
42 T. Tang, C. Liu, Z. Min, W. Cai, X. Zhang and W. Li, *et al.*, Microfluidic Fabrication of Gelatin Acrylamide Microgels through Visible Light Photopolymerization for Cell Encapsulation, *ACS Appl. Bio Mater.*, 2023, **6**(6), 2496–2504.
43 T. Billiet, E. Gevaert, T. De Schryver, M. Cornelissen and P. Dubruel, The 3D printing of gelatin methacrylamide cell-laden tissue-engineered constructs with high cell viability, *Biomaterials*, 2014, **35**(1), 49–62.

44 P. Occhetta, R. Visone, L. Russo, L. Cipolla, M. Moretti and M. Rasponi, VA-086 methacrylate gelatine photopolymerizable hydrogels: A parametric study for highly biocompatible 3D cell embedding, *J. Biomed. Mater. Res., Part A*, 2015, **103**(6), 2109–2117.

45 A. Chih-Hsin Lin, K. F. Lin, K. Mar, S. Y. Lee and Y. M. Lin, *Antioxidant N-Acetylcysteine and Glutathione Increase the Viability and Proliferation of MG63 Cells Encapsulated in the Gelatin Methacrylate/VA-086/Blue Light Hydrogel System FULL TEXT*.

46 Z. Wang, R. Abdulla, B. Parker, R. Samanipour, S. Ghosh and K. Kim, A simple and high-resolution stereolithography-based 3D bioprinting system using visible light crosslinkable bioinks, *Biofabrication*, 2015, **7**(4), 045009.

47 H. Shih and C. C. Lin, Visible-light-mediated thiol-ene hydrogelation using eosin-Y as the only photoinitiator, *Macromol. Rapid Commun.*, 2013, **34**(3), 269–273.

48 S. Sharifi, H. Sharifi, A. Akbari and J. Chodosh, Systematic optimization of visible light-induced crosslinking conditions of gelatin methacryloyl (GelMA), *Sci. Rep.*, 2021, **11**(1), 23276.

49 I. Noshadi, S. Hong, K. E. Sullivan, E. Shirzaei Sani, R. Portillo-Lara and A. Tamayol, *et al.*, In vitro and in vivo analysis of visible light crosslinkable gelatin methacryloyl (GelMA) hydrogels, *Biomater. Sci.*, 2017, **5**(10), 2093–2105.

50 E. Andrzejewska, D. Zych-Tomkowiak, M. Andrzejewski, G. L. Hug and B. Marciniak, Heteroaromatic thiols as coinitiators for type II photoinitiating systems based on camphorquinone and isopropylthioxanthone, *Macromolecules*, 2006, **39**(11), 3777–3785.

51 A. A. Pérez-Mondragón, C. E. Cuevas-Suárez, J. A. González-López, N. Trejo-Carbajal and A. M. Herrera-González, Evaluation of new coinitiators of camphorquinone useful in the radical photopolymerization of dental monomers, *J. Photochem. Photobiol., A*, 2020, 403.

52 J. Hu, Y. Hou, H. Park, B. Choi, S. Hou and A. Chung, *et al.*, Visible light crosslinkable chitosan hydrogels for tissue engineering, *Acta Biomater.*, 2012, **8**(5), 1730–1738.

53 S. You, J. Li, W. Zhu, C. Yu, D. Mei and S. Chen, Nanoscale 3D printing of hydrogels for cellular tissue engineering, *J. Mater. Chem. B*, 2018, **6**(15), 2187–2197.

54 J. Torgersen, A. Ovsianikov, V. Mironov, N. Pucher, X. Qin and Z. Li, *et al.*, Photo-sensitive hydrogels for three-dimensional laser microfabrication in the presence of whole organisms, *J. Biomed. Opt.*, 2012, **17**(10), 105008.

55 X. H. Qin, J. Torgersen, R. Saf, S. Mühleder, N. Pucher and S. C. Ligon, *et al.*, Three-dimensional microfabrication of protein hydrogels via two-photon-excited thiol-vinyl ester photopolymerization, *J. Polym. Sci., Part A: Gen. Pap.*, 2013, **51**(22), 4799–4810.

56 A. Ovsianikov, S. Mühleder, J. Torgersen, Z. Li, X. H. Qin and S. Van Vlierberghe, *et al.*, Laser photofabrication of cell-containing hydrogel constructs, *Langmuir*, 2014, **30**(13), 3787–3794.

57 K. Taki, Y. Watanabe, H. Ito and M. Ohshima, Effect of oxygen inhibition on the kinetic constants of the UV-radical photopolymerization of diurethane dimethacrylate/photoinitiator systems, *Macromolecules*, 2014, **47**(6), 1906–1913.

58 A. Sun, X. He, X. Ji, D. Hu, M. Pan and L. Zhang, *et al.*, Current research progress of photopolymerized hydrogels in tissue engineering, *Chin. Chem. Lett.*, 2021, **32**(7), 2117–2126.

59 N. E. Fedorovich, M. H. Oudshoorn, D. van Geemen, W. E. Hennink, J. Alblas and W. J. A. Dhert, The effect of photopolymerization on stem cells embedded in hydrogels, *Biomaterials*, 2009, **30**(3), 344–353.

60 B. D. Fairbanks, M. P. Schwartz, C. N. Bowman and K. S. Anseth, Photoinitiated polymerization of PEG-diacrylate with lithium phenyl-2,4,6-trimethylbenzoylphosphinate: polymerization rate and cytocompatibility, *Biomaterials*, 2009, **30**(35), 6702–6707.

61 H. Xu, J. Casillas, S. Krishnamoorthy and C. Xu, Effects of Irgacure 2959 and lithium phenyl-2,4,6-trimethylbenzoylphosphinate on cell viability, physical properties, and microstructure in 3D bioprinting of vascular-like constructs, *Biomed. Mater.*, 2020, **15**(5), 055021.

62 S. B. Gugulothu and K. Chatterjee, Visible Light-Based 4D-Bioprinted Tissue Scaffold, *ACS Macro Lett.*, 2023, **12**(4), 494–502.

63 M. D. Goodner and C. N. Bowman, Modeling primary radical termination and its effects on autoacceleration in photopolymerization kinetics, *Macromolecules*, 1999, **32**(20), 6552–6559.

64 H. Kumar, K. Sakthivel, M. G. A. Mohamed, E. Boras, S. R. Shin and K. Kim, Designing Gelatin Methacryloyl (GelMA)-Based Bioinks for Visible Light Stereolithographic 3D Biofabrication, *Macromol. Biosci.*, 2021, **21**(1), 2000317.

65 R. Goto, E. Nishida, S. Kobayashi, M. Aino, T. Ohno and Y. Iwamura, *et al.*, Gelatin methacryloyl–riboflavin (Gelma–rf) hydrogels for bone regeneration, *Int. J. Mol. Sci.*, 2021, **22**(4), 1–12.

66 J. Y. Lee and G. H. Kim, A cryopreservable cell-laden GelMa-based scaffold fabricated using a 3D printing process supplemented with an in situ photo-crosslinking, *J. Ind. Eng. Chem.*, 2020, **85**, 249–257.

67 H. He, L. Li and L. J. Lee, Photopolymerization and structure formation of methacrylic acid based hydrogels: The effect of light intensity, *React. Funct. Polym.*, 2008, **68**(1), 103–113.

68 M. Y. Shie, J. J. Lee, C. C. Ho, S. Y. Yen, H. Y. Ng and Y. W. Chen, Effects of gelatin methacrylate bio-ink concentration on mechano-physical properties and human dermal fibroblast behavior, *Polymers*, 2020, **12**(9), 1930.

69 Y. Wu, Y. Xiang, J. Fang, X. Li, Z. Lin and G. Dai, *et al.*, The influence of the stiffness of GelMA substrate on the outgrowth of PC12 cells, *Biosci. Rep.*, 2019, **39**(1), BSR20181748.

70 A. I. van den Bulcke, B. Bogdanov, N. de Rooze, E. H. Schacht, M. Cornelissen and H. Berghmans,

Structural and rheological properties of methacrylamide modified gelatin hydrogels, *Biomacromolecules*, 2000, **1**(1), 31–38.

71 S. Krishnamoorthy, B. Noorani and C. Xu, Effects of encapsulated cells on the physical–mechanical properties and microstructure of gelatin methacrylate hydrogels, *Int. J. Mol. Sci.*, 2019, **20**(20), 5061.

72 M. Sun, X. Sun, Z. Wang, S. Guo, G. Yu and H. Yang, Synthesis and properties of gelatin methacryloyl (GelMA) hydrogels and their recent applications in load-bearing tissue, *Polymers*, 2018, **10**, 1290.

73 B. H. Lee, H. Shirahama, N. J. Cho and L. P. Tan, Efficient and controllable synthesis of highly substituted gelatin methacrylamide for mechanically stiff hydrogels, *RSC Adv.*, 2015, **5**(128), 106094–106097.

74 B. H. Lee, N. Lum, L. Y. Seow, P. Q. Lim and L. P. Tan, Synthesis and characterization of types A and B gelatin methacryloyl for bioink applications, *Materials*, 2016, **9**(10), 797.

75 H. Shirahama, B. H. Lee, L. P. Tan and N. J. Cho, Precise tuning of facile one-pot gelatin methacryloyl (GelMA) synthesis, *Sci. Rep.*, 2016, 6.

76 D. Loessner, C. Meinert, E. Kaemmerer, L. C. Martine, K. Yue and P. A. Levett, *et al.*, Functionalization, preparation and use of cell-laden gelatin methacryloyl-based hydrogels as modular tissue culture platforms, *Nat. Protoc.*, 2016, **11**(4), 727–746.

77 M. Kirsch, L. Birnstein, I. Pepelanova, W. Handke, J. Rach and A. Seltsam, *et al.*, Gelatin-Methacryloyl (GelMA) Formulated with Human Platelet Lysate Supports Mesenchymal Stem Cell Proliferation and Differentiation and Enhances the Hydrogel's Mechanical Properties, *Bioengineering*, 2019, **6**(3), 76.

78 C. Claaßen, M. H. Claaßen, V. Truffault, L. Sewald, G. E. M. Tovar and K. Borchers, *et al.*, Quantification of Substitution of Gelatin Methacryloyl: Best Practice and Current Pitfalls, *Biomacromolecules*, 2018, **19**(1), 42–52.

79 J. M. Zatorski, A. N. Montalbine, J. E. Ortiz-Cárdenas and R. R. Pompano, Quantification of fractional and absolute functionalization of gelatin hydrogels by optimized ninhydrin assay and 1H NMR, *Anal. Bioanal. Chem.*, 2020, **412**(24), 6211–6220.

80 G. Ying, N. Jiang, C. Yu and Y. S. Zhang, Three-dimensional bioprinting of gelatin methacryloyl (GelMA)., *Bio-Des. Manuf.*, 2018, **1**, 215–224.

81 L. Ning, R. Mehta, C. Cao, A. Theus, M. Tomov and N. Zhu, *et al.*, Embedded 3D Bioprinting of Gelatin Methacryloyl-Based Constructs with Highly Tunable Structural Fidelity, *ACS Appl. Mater. Interfaces*, 2020, **12**(40), 44563–44577.

82 N. Annabi, J. W. Nichol, X. Zhong, C. Ji, S. Koshy, A. Khademhosseini and F. Dehghani, Controlling the Porosity and Microarchitecture of Hydrogels for Tissue Engineering, *Tissue Eng., Part B*, 2010, **16**(4), 371–383.

83 S. Y. Jo, J. U. Lee, H. Lee, D. Ryu and G. H. Kim, The one-step fabrication of porous hASC-laden GelMa constructs using a handheld printing system, *npj Regener. Med.*, 2023, **8**(1), 30.

84 S. R. Ur Rehman, R. Augustine, A. A. Zahid, R. Ahmed, M. Tariq and A. Hasan, Reduced graphene oxide incorporated gelma hydrogel promotes angiogenesis for wound healing applications, *Int. J. Nanomed.*, 2019, **14**, 9603–9617.

85 M. Shi, Q. Xu, L. Ding, Y. Xia, C. Zhang and H. Lai, *et al.*, Cell Infiltrative Inner Connected Porous Hydrogel Improves Neural Stem Cell Migration and Differentiation for Functional Repair of Spinal Cord Injury, *ACS Biomater. Sci. Eng.*, 2022, **8**(12), 5307–5318.

86 P. Song, M. Li, B. Zhang, X. Gui, Y. Han and L. Wang, *et al.*, DLP fabricating of precision GelMA/HAp porous composite scaffold for bone tissue engineering application, *Composites, Part B*, 2022, **244**, 110163.

87 T. Dursun Usal, D. Yucel and V. Hasirci, A novel GelMA-pHEMA hydrogel nerve guide for the treatment of peripheral nerve damages, *Int. J. Biol. Macromol.*, 2019, **121**, 699–706.

88 Z. Yang, X. Ren and Y. Liu, Multifunctional 3D printed porous GelMA/xanthan gum based dressing with biofilm control and wound healing activity, *Mater. Sci. Eng., C*, 2021, 131.

89 H. Kamata and X. Li, Chung U Il, Sakai T. Design of Hydrogels for Biomedical Applications, *Adv. Healthcare Mater.*, 2015, **4**(16), 2360–2374.

90 N. S. Kulkarni, G. Chauhan, M. Goyal, S. Sarvepalli and V. Gupta, Development of gelatin methacrylate (GelMa) hydrogels for versatile intracavitary applications, *Biomater. Sci.*, 2022, **10**(16), 4492–4507.

91 G. Basara, X. Yue and P. Zorlutuna, Dual crosslinked gelatin methacryloyl hydrogels for photolithography and 3D printing, *Gels*, 2019, **5**(3), 34.

92 M. Rizwan, G. S. L. Peh, H. P. Ang, N. C. Lwin, K. Adnan and J. S. Mehta, *et al.*, Sequentially-crosslinked bioactive hydrogels as nano-patterned substrates with customizable stiffness and degradation for corneal tissue engineering applications, *Biomaterials*, 2017, **120**, 139–154. Available from: **https://www.sciencedirect.com/science/article/pii/S0142961216307372**.

93 M. Zhu, Y. Wang, G. Ferracci, J. Zheng, N. J. Cho and B. H. Lee, Gelatin methacryloyl and its hydrogels with an exceptional degree of controllability and batch-to-batch consistency, *Sci. Rep.*, 2019, **9**(1), 6838.

94 P. Kim, A. Yuan, K. H. Nam, A. Jiao and D. H. Kim, Fabrication of poly(ethylene glycol): Gelatin methacrylate composite nanostructures with tunable stiffness and degradation for vascular tissue engineering, *Biofabrication*, 2014, **6**(2), 024112.

95 S. M. Bittner, H. A. Pearce, K. J. Hogan, M. M. Smoak, J. L. Guo and A. J. Melchiorri, *et al.*, Swelling Behaviors of 3D Printed Hydrogel and Hydrogel-Microcarrier Composite Scaffolds, *Tissue Eng., Part A*, 2021, **27**(11–12), 665–678.

96 A. T. Young, O. C. White and M. A. Daniele, Rheological Properties of Coordinated Physical Gelation and Chemical Crosslinking in Gelatin Methacryloyl (GelMA) Hydrogels, *Macromol. Biosci.*, 2020, **20**(12), 2000183.

97 T. Billiet, M. Vandenhaute, J. Schelfhout, S. Van Vlierberghe and P. Dubruel, A review of trends and

limitations in hydrogel-rapid prototyping for tissue engineering, *Biomaterials*, 2012, **33**(26), 6020–6041. Available from: https://www.sciencedirect.com/science/article/pii/S0142961212004899.

98 H. Hwangbo, H. Lee, E. J. Jin, J. Y. Lee, Y. Jo and D. Ryu, *et al.*, Bio-printing of aligned GelMa-based cell-laden structure for muscle tissue regeneration, *Bioact. Mater.*, 2022, **8**, 57–70.

99 J. P. Joseph, S. B. Gugulothu, D. Nandi and K. Chatterjee, Mechanical Properties Affect Primary T Cell Activation in 3D Bioprinted Hydrogels, *ACS Macro Lett.*, 2023, 1085–1093.

100 H. Wang, L. Zhou, J. Liao, Y. Tan, K. Ouyang and C. Ning, *et al.*, Cell-laden photocrosslinked GelMA-DexMA copolymer hydrogels with tunable mechanical properties for tissue engineering, *J. Mater. Sci.: Mater. Med.*, 2014, **25**(9), 2173–2183.

101 B. J. Klotz and D. Gawlitta, Rosenberg AJWP, Malda J, Melchels FPW. Gelatin-Methacryloyl Hydrogels: Towards Biofabrication-Based Tissue Repair, *Trends Biotechnol.*, 2016, **34**, 394–407.

102 T. A. Arica, M. Guzelgulgen, A. A. Yildiz and M. M. Demir, Electrospun GelMA fibers and p(HEMA) matrix composite for corneal tissue engineering, *Mater. Sci. Eng., C*, 2021, **120**, 111720.

103 J. H. Wang, C. W. Tsai, N. Y. Tsai, C. Y. Chiang, R. S. Lin and R. F. Pereira, *et al.*, An injectable, dual crosslinkable hybrid pectin methacrylate (PECMA)/gelatin methacryloyl (GelMA) hydrogel for skin hemostasis applications, *Int. J. Biol. Macromol.*, 2021, **185**, 441–450.

104 M. Tavafoghi, A. Sheikhi, R. Tutar, J. Jahangiry, A. Baidya and R. Haghniaz, *et al.*, Engineering Tough, Injectable, Naturally Derived, Bioadhesive Composite Hydrogels, *Adv. Healthcare Mater.*, 2020, **9**(10), 1–12.

105 L. Han, J. Xu, X. Lu, D. Gan, Z. Wang and K. Wang, *et al.*, Biohybrid methacrylated gelatin/polyacrylamide hydrogels for cartilage repair, *J. Mater. Chem. B*, 2017, **5**(4), 731–741.

106 A. A. Aldana, F. Valente, R. Dilley and B. Doyle, Development of 3D bioprinted GelMA-alginate hydrogels with tunable mechanical properties, *Bioprinting*, 2021, **21**, e00105.

107 S. Ahadian, S. Yamada, J. Ramón-Azcón, M. Estili, X. Liang and K. Nakajima, *et al.*, Hybrid hydrogel-aligned carbon nanotube scaffolds to enhance cardiac differentiation of embryoid bodies, *Acta Biomater.*, 2016, **31**, 134–143.

108 J. M. Unagolla and A. C. Jayasuriya, Hydrogel-based 3D bioprinting: A comprehensive review on cell-laden hydrogels, bioink formulations, and future perspectives, *Appl Mater. Today*, 2020, **18**, 100479. Available from: https://www.sciencedirect.com/science/article/pii/S2352940719305980.

109 R. Pantani and L. S. Turng, Manufacturing of advanced biodegradable polymeric components, *J. Appl. Polym. Sci.*, 2015, (48), 132, DOI: 10.1002/app.42889. Available from: .

110 J. Li, C. Wu, P. K. Chu and M. Gelinsky, 3D printing of hydrogels: Rational design strategies and emerging biomedical applications, *Mater. Sci. Eng., R*, 2020, **140**, 100543. Available from: https://www.sciencedirect.com/science/article/pii/S0927796X20300012.

111 L. R. Chang, G. Marston and A. Martin, Anatomy, Cartilage, 2021.

112 E. Kheir and D. Shaw, Hyaline articular cartilage, *Orthop. Traumatol.*, 2009, **23**(6), 450–455.

113 J. Lowe and A. J. Almarza, A review of in-vitro fibrocartilage tissue engineered therapies with a focus on the temporomandibular joint, *Arch. Oral Biol.*, 2017, **83**, 193–201.

114 Y. Krishnan and A. J. Grodzinsky, Cartilage diseases, *Matrix Biology*, Elsevier B.V., 2018, vol. 71–72, pp. 51–69.

115 H. Kwon, W. E. Brown, C. A. Lee, D. Wang, N. Paschos and J. C. Hu, *et al.*, Surgical and tissue engineering strategies for articular cartilage and meniscus repair, *Nat. Rev. Rheumatol.*, 2019, **15**(9), 550–570, DOI: 10.1038/s41584-019-0255-1.

116 K. L. Spiller, S. A. Maher and A. M. Lowman, Hydrogels for the repair of articular cartilage defects, *Tissue Eng., Part B*, 2011, **17**(4), 281–299.

117 X. Li, S. Chen, J. Li, X. Wang, J. Zhang and N. Kawazoe, *et al.*, 3D culture of chondrocytes in gelatin hydrogels with different stiffness, *Polymers*, 2016, **8**(8), 269.

118 X. Li, Y. Chen, N. Kawazoe and G. Chen, Influence of microporous gelatin hydrogels on chondrocyte functions, *J. Mater. Chem. B*, 2017, **5**(29), 5753–5762.

119 A. C. Daly, F. E. Freeman, T. Gonzalez-Fernandez, S. E. Critchley, J. Nulty and D. J. Kelly, 3D Bioprinting for Cartilage and Osteochondral Tissue Engineering, *Adv. Healthcare Mater.*, 2017, **6**(22), 1700298, DOI: 10.1002/adhm.201700298.

120 W. Zhu, H. Cui, B. Boualam, F. Masood, E. Flynn and R. D. Rao, *et al.*, 3D bioprinting mesenchymal stem cell-laden construct with core-shell nanospheres for cartilage tissue engineering, *Nanotechnology*, 2018, **29**(18), 185101.

121 G. Gao, A. F. Schilling, K. Hubbell, T. Yonezawa, D. Truong and Y. Hong, *et al.*, Improved properties of bone and cartilage tissue from 3D inkjet-bioprinted human mesenchymal stem cells by simultaneous deposition and photocrosslinking in PEG-GelMA, *Biotechnol. Lett.*, 2015, **37**(11), 2349–2355, DOI: 10.1007/s10529-015-1921-2.

122 M. Costantini, J. Idaszek, K. Szöke, J. Jaroszewicz, M. Dentini and A. Barbetta, *et al.*, 3D bioprinting of BM-MSCs-loaded ECM biomimetic hydrogels for in vitro neocartilage formation, *Biofabrication*, 2016, **8**(3), 35002, DOI: 10.1088/1758-5090/8/3/035002.

123 J. Gao, X. Ding, X. Yu, X. Chen, X. Zhang and S. Cui, *et al.*, Cell-Free Bilayered Porous Scaffolds for Osteochondral Regeneration Fabricated by Continuous 3D-Printing Using Nascent Physical Hydrogel as Ink, *Adv. Healthcare Mater.*, 2021, **10**(3), 2001404.

124 L. Ruiz-Cantu, A. Gleadall, C. Faris, J. Segal, K. Shakesheff and J. Yang, Multi-material 3D bioprinting of porous constructs for cartilage regeneration, *Mater. Sci. Eng., C*, 2020, 109.

125 M. J. Olszta, X. Cheng, S. S. Jee, R. Kumar, Y. Y. Kim and M. J. Kaufman, *et al.*, Bone structure and formation: A new perspective, *Mater. Sci. Eng., R*, 2007, **58**(3–5), 77–116.

126 M. Askari, M. Afzali Naniz, M. Kouhi, A. Saberi, A. Zolfagharian and M. Bodaghi, Recent progress in extrusion 3D bioprinting of hydrogel biomaterials for tissue regeneration: a comprehensive review with focus on advanced fabrication techniques, *Biomater. Sci.*, 2021, **9**(3), 535–573.

127 B. Byambaa, N. Annabi, K. Yue, S. G. Trujillo-de, M. M. Alvarez and W. Jia, *et al.*, Bioprinted Osteogenic and Vasculogenic Patterns for Engineering 3D Bone Tissue, *Adv. Healthcare Mater.*, 2017, **6**(16), 1700015.

128 S. Buyuksungur, V. Hasirci and N. Hasirci, 3D printed hybrid bone constructs of PCL and dental pulp stem cells loaded GelMA, *J. Biomed. Mater. Res., Part A*, 2021, **109**(12), 2425–2437.

129 P. Camelliti, T. Borg and P. Kohl, Structural and functional characterisation of cardiac fibroblasts, *Cardiovasc. Res.*, 2005, **65**(1), 40–51.

130 N. B. Allen, B. Abar, L. Johnson, J. Burbano, R. M. Danilkowicz and S. B. Adams, 3D-bioprinted GelMA-gelatin-hydroxyapatite osteoblast-laden composite hydrogels for bone tissue engineering, *Bioprinting*, 2022, **26**, e00196.

131 G. Cidonio, C. R. Alcala-Orozco, K. S. Lim, M. Glinka, I. Mutreja and Y. H. Kim, *et al.*, Osteogenic and angiogenic tissue formation in high fidelity nanocomposite Laponite-gelatin bioinks, *Biofabrication*, 2019, **11**(3), 035027.

132 O. Monfredi, H. Dobrzynski, T. Mondal., R. Boyett Mark and G. M. Morris, The Anatomy and Physiology of the Sinoatrial Node-A Contemporary Review, *Pacing Clin. Electrophysiol.*, 2010, **33**(11), 1392–1406.

133 Z. Wang, L. Wang, T. Li, S. Liu, B. Guo and W. Huang, *et al.*, 3D bioprinting in cardiac tissue engineering, *Theranostics*, 2021, **11**(16), 7948–7969.

134 T. Agarwal, G. M. Fortunato, S. Y. Hann, B. Ayan, K. Y. Vajanthri and D. Presutti, *et al.*, Recent advances in bioprinting technologies for engineering cardiac tissue, *Mater. Sci. Eng., C*, 2021, **124**, 112057.

135 B. Duan, E. Kapetanovic, L. A. Hockaday and J. T. Butcher, Three-dimensional printed trileaflet valve conduits using biological hydrogels and human valve interstitial cells, *Acta Biomater.*, 2014, **10**(5), 1836–1846.

136 D. Bejleri, B. W. Streeter, A. L. Y. Nachlas, M. E. Brown, R. Gaetani and K. L. Christman, *et al.*, A Bioprinted Cardiac Patch Composed of Cardiac-Specific Extracellular Matrix and Progenitor Cells for Heart Repair, *Adv. Healthcare Mater.*, 2018, **7**(23), 1800672.

137 K. Zhu, S. R. Shin, T. van Kempen, Y. Li, V. Ponraj and A. Nasajpour, *et al.*, Gold Nanocomposite Bioink for Printing 3D Cardiac Constructs, *Adv. Funct. Mater.*, 2017, **27**(12), 1605352.

138 M. Buckingham, L. Bajard, T. Chang, P. Daubas, J. Hadchouel and S. Meilhac, *et al.*, The formation of skeletal muscle: from somite to limb, *J. Anat.*, 2003, **202**(1), 59–68.

139 W. R. Frontera and J. Ochala, Skeletal Muscle: A Brief Review of Structure and Function, *Calcif. Tissue Int.*, 2015, **96**(3), 183–195.

140 M. M. Smoak and A. G. Mikos, Advances in biomaterials for skeletal muscle engineering and obstacles still to overcome, *Mater. Today Bio*, 2020, **7**, 100069.

141 W. Kim and G. Kim, 3D bioprinting of functional cell-laden bioinks and its application for cell-alignment and maturation, *Appl Mater. Today*, 2020, **19**, 100588.

142 A. García-Lizarribar, X. Fernández-Garibay, F. Velasco-Mallorquí, A. G. Castaño, J. Samitier and J. Ramon-Azcon, Composite Biomaterials as Long-Lasting Scaffolds for 3D Bioprinting of Highly Aligned Muscle Tissue, *Macromol. Biosci.*, 2018, **18**(10), 1800167.

143 S. Böttcher-Haberzeth, T. Biedermann and E. Reichmann, Tissue engineering of skin, *Burns.*, 2010, **36**(4), 450–460.

144 Ç.-S. Seyedmahmoud, N. Barros and S. Banton, *et al.*, Three-Dimensional Bioprinting of Functional Skeletal Muscle Tissue Using GelatinMethacryloyl-Alginate Bioinks, *Micromachines*, 2019, **10**(10), 679.

145 M. Ponec, Skin constructs for replacement of skin tissues for in vitro testing, *Adv. Drug Delivery Rev.*, 2002, **54**, S19–S30.

146 R. L. Eckert, Structure, function, and differentiation of the keratinocyte, *Physiol. Rev.*, 1989, **69**(4), 1316–1346.

147 F. Fayyazbakhsh and M. C. Leu, A Brief Review on 3D Bioprinted Skin Substitutes, *Procedia Manuf.*, 2020, **48**, 790–796.

148 Y. Shi, T. L. Xing, H. B. Zhang, R. X. Yin, S. M. Yang and J. Wei, *et al.*, Tyrosinase-doped bioink for 3D bioprinting of living skin constructs, *Biomed. Mater.*, 2018, **13**(3), 035008.

149 W. Xu, B. Z. Molino, F. Cheng, P. J. Molino, Z. Yue and D. Su, *et al.*, On Low-Concentration Inks Formulated by Nanocellulose Assisted with Gelatin Methacrylate (GelMA) for 3D Printing toward Wound Healing Application, *ACS Appl. Mater. Interfaces*, 2019, **11**(9), 8838–8848.

150 R. Jin, Y. Cui, H. Chen, Z. Zhang, T. Weng and S. Xia, *et al.*, Three-dimensional bioprinting of a full-thickness functional skin model using acellular dermal matrix and gelatin methacrylamide bioink, *Acta Biomater.*, 2021, **131**, 248–261.

151 J. Zeng, L. Jia, D. Wang, Z. Chen, W. Liu and Q. Yang, *et al.*, Bacterial nanocellulose-reinforced gelatin methacryloyl hydrogel enhances biomechanical property and glycosaminoglycan content of 3D-bioprinted cartilage, *Int. J. Bioprint.*, 2023, **9**(1), 131–143.

152 X. Gui, Z. Peng, P. Song, L. Chen, X. Xu and H. Li, *et al.*, 3D printing of personalized polylactic acid scaffold laden with GelMA/autologous auricle cartilage to promote ear reconstruction, *Biodes Manuf.*, 2023, 1–13.

153 J. Chakraborty, J. Fernández-Pérez, K. A. Van Kampen, S. Roy, T. Ten Brink and C. Mota, *et al.*, Development of a biomimetic arch-like 3D bioprinted construct for cartilage regeneration using gelatin methacryloyl and silk fibroin-gelatin bioinks, *Biofabrication*, 2023, **15**(3), 035009.

154 R. L. Alexa, A. Cucuruz, C. D. Ghiţulică, G. Voicu, L. R. Stamat and S. Dinescu, *et al.*, 3D Printable Composite Biomaterials Based on GelMA and Hydroxyapatite Powders Doped with Cerium Ions for Bone Tissue Regeneration, *Int. J. Mol. Sci.*, 2022, **23**(3), 1841.

155 Z. Li, S. Li, J. Yang, Y. Ha, Q. Zhang and X. Zhou, *et al.*, 3D bioprinted gelatin/gellan gum-based scaffold with double-crosslinking network for vascularized bone regeneration, *Carbohydr. Polym.*, 2022, **290**, 119469. Available from: https://www.sciencedirect.com/science/article/pii/S0144861722003745.

156 X. Zhang, H. Zhang, Y. Zhang, H. Huangfu, Y. Yang and Q. Qin, *et al.*, 3D printed reduced graphene oxide-GelMA hybrid hydrogel scaffolds for potential neuralized bone regeneration, *J. Mater. Chem. B*, 2023, **11**(6), 1288–1301, DOI: 10.1039/D2TB01979E.

157 G. Basara, S. Gulberk Ozcebe, B. W. Ellis and P. Zorlutuna, Tunable human myocardium derived decellularized extracellular matrix for 3d bioprinting and cardiac tissue engineering, *Gels*, 2021, **7**(2), 70.

158 M. E. Kupfer, W. H. Lin, V. Ravikumar, K. Qiu, L. Wang and L. Gao, *et al.*, In Situ Expansion, Differentiation, and Electromechanical Coupling of Human Cardiac Muscle in a 3D Bioprinted, Chambered Organoid, *Circ. Res.*, 2020, **127**(2), 207–224.

159 D. C. van der Valk, C. F. T. van der Ven, M. C. Blaser, J. M. Grolman, P. J. Wu and O. S. Fenton, *et al.*, Engineering a 3d-bioprinted model of human heart valve disease using nanoindentation-based biomechanics, *Nanomaterials*, 2018, **8**(5), 296.

160 J. Y. Lee, H. Lee, E. J. Jin, D. Ryu and G. H. Kim, 3D bioprinting using a new photo-crosslinking method for muscle tissue restoration, *npj Regener. Med.*, 2023, **8**(1), 18.

161 T. Li, J. Hou, L. Wang, G. Zeng, Z. Wang and L. Yu, *et al.*, Bioprinted anisotropic scaffolds with fast stress relaxation bioink for engineering 3D skeletal muscle and repairing volumetric muscle loss, *Acta Biomater.*, 2023, **156**, 21–36.

162 A. García-Lizarribar, A. Villasante, J. A. Lopez-Martin, M. Flandez, M. C. Soler-Vázquez and D. Serra, *et al.*, 3D bioprinted functional skeletal muscle models have potential applications for studies of muscle wasting in cancer cachexia, *Biomater. Adv.*, 2023, 150.

163 L. Xu, Z. Zhang, A. M. Jorgensen, Y. Yang, Q. Jin and G. Zhang, *et al.*, Bioprinting a skin patch with dual-crosslinked gelatin (GelMA) and silk fibroin (SilMA): An approach to accelerating cutaneous wound healing, *Mater. Today Bio*, 2023, 18.

164 M. Li, L. Sun, Z. Liu, Z. Shen, Y. Cao and L. Han, *et al.*, 3D bioprinting of heterogeneous tissue-engineered skin containing human dermal fibroblasts and keratinocytes, *Biomater. Sci.*, 2023, **11**(7), 2461–2477.

165 D. Zhang, Q. Fu, H. Fu, J. Zeng, L. Jia and M. Chen, 3D-bioprinted human lipoaspirate-derived cell-laden skin constructs for healing of full-thickness skin defects, *Int. J. Bioprint.*, 2023, **9**(4), DOI: 10.18063/ijb.718.